*Relationship between GNAS gene expression and PFS*

Of the 107 independent samples, RNA from 62 was available for real-time RT-PCR analysis. There are no significant associations between GNAS expression and clinical factors such as age, histological grade, and operation status. GNAS expression correlates significantly with PFS of aEOC ($p = 0.03$) (Fig. 2B).

## Discussion

The platinum/taxane regimen has improved the prognosis of EOC; however, this remains poor. For this reason, it is very important to find new prognostic markers for EOC receiving standard therapy, so that future clinical trials can be focused on patients with a poor prognosis. In this study, we used oligonucleotide microarrays to identify new prognostic biomarkers for aEOC excluding clear cell or mucinous types receiving standard therapy. In the past decade, several studies have analyzed chromosomal imbalances using comparative genomic hybridization (CGH) in EOC [10,17–20]. Arnold et al. investigated 47 malignant ovarian tumors and 2 ovarian tumors of low malignant potential using CGH and demonstrated that common genetic changes include DNA gains of chromosome arms 8q24 (51%) and 20q13.2-qter (40%) [10]. Iwabuchi et al. presented CGH data from 31 ovarian carcinomas and reported that increased copy numbers were most commonly observed in their cases at 3q26 (42%), 8q24 (35%), and 12q11.1–12 (25%) [17], while Sonoda et al. demonstrated that the most frequent sites of copy number increase were 8q24.1 (56%) and 20q13.2-qter (48%) in tumor DNA from 25 malignant ovarian carcinomas and 2 tumors of low malignant potential [18]. Tanner et al. focused on 20q12–q13 amplification in 24 sporadic, 3 familial and 4 hereditary ovarian carcinomas, and 8 ovarian cancer cell lines [19]. They demonstrated high-level amplification of at least one of the five non-syntenic regions at 20q12–q13.2 in 13 sporadic (54%) and in all four hereditary tumors [19]. Hu et al. focused on ovarian serous carcinomas and demonstrated DNA copy number gain at 8q22q24 and 20q12q13 in 60% and 45% of samples, respectively [20] In our study, amplification rates of GNAS at 20q13 is 30%, respectively.

Furthermore, Tanner et al. showed a tendency toward correlation between amplification and poor survival (not significant) and Hu et al. reported that 20q12q13 amplification may indicate a high risk for recurrence of serous ovarian cancer [19,20]. These reports included various histologic types and stages and even cell lines as well as primary and recurrent cases. Furthermore, they provide no information on therapy or operation status, include small number of patients, and do not perform validation assays. As it is well established that patients with ovarian carcinoma of different histologic types vary in their response to chemotherapy [8,9], it is important to take this into account in testing new biomarkers for their utility in clinical practice. In this study therefore, we focused on patients receiving standard therapy, excluding those with mucinous and clear cell tumors, and performed microarray analysis in 33 patients and validation assays in 107 patients.

Recent attempts to develop accurate predictors of clinical outcome in ovarian cancer have focused on techniques that are capable of assessing global gene status such as expression profiling and array CGH [4–7]. Birrer et al. performed oligonucleotide array CGH on 42 microdissected high-grade serous ovarian tumors and reported that amplification at 5q31–5q35.3 exhibited the strongest correlation with overall survival, identifying FGF-1 on 5q31 as a prognostic marker in 81 independent samples [7]. These data are not in agreement with our own. However, Birrer et al.'s report provides no information about the chemotherapy used, so that we speculate that prognostic biomarkers may be dependent on the chemotherapeutic regimen. Spentzos et al. also reported expression profiles for EOC and established a Chemotherapy Response Profile (CRP) and Ovarian Cancer Prognostic Profile (OCPP) [4,6].

We selected GNAS gene based on the $p$ value and fold change in array data and examined the amplification status of GNAS as prognostic marker of aEOC. GNAS gene amplification was an independent prognostic factor. The GNAS locus encodes the G (alpha) protein, which stimulates the formation of cyclic AMP (cAMP). The cAMP pathway mediates pleiotropic effects including regulation of apoptosis and proliferation [21–23] and different genotypes of the single nucleotide polymorphism (ANP) T393C in the GNAS gene predict the clinical outcóme of urothelial carcinoma, sporadic colorectal cancer, renal cell carcinoma, and chronic lymphocytic leukemia [24–27]. However, the role of GNAS in EOC remains unclear.

In conclusion, we identified amplification of GNAS on 20q13 as markers of prognosis in patients with aEOC treated with standard therapy. Our finding identifies qualitative and reproducible biomarker to predict the PFS of aEOC.

**Conflict of interest statement**

All of the authors are aware of and agree to the content of the article and have no conflict interest.

## Acknowledgments

The authors are grateful to Asami Nagata, Kanako Matsumoto, and Nozomi Tsuji for their technical assistance. This study was supported in part by a Grant-in-Aid for Scientific Research on Priority Areas from the Ministry of Education, Science and Culture, Japan (20014024), A Grant-in Aid for scientific Research (C) from the Ministry of Education, Science and Culture, Japan (19591940), and a grant from Osaka City General Hospital.

## References

[1] Ben David Y, Chetrit A, Hirsh-Yechezkel G, Friedman E, Beck BD, Beller U, et al. Effect of BRCA mutations on the length of survival in epithelial ovarian tumors. J Clin Oncol 2002;20(2):463–6.
[2] Tai YT, Lee S, Niloff E, Weisman C, Strobel T, Cannistra SA. BAX protein expression and clinical outcome in epithelial ovarian cancer. J Clin Oncol 1998;16(8):2583–90.
[3] Kusume T, Tsuda H, Kawabata M, Inoue T, Umesaki N, Suzuki T, et al. The p16-cyclin D1/CDK4-pRb pathway and clinical outcome in epithelial ovarian cancer. Clin Cancer Res 1999;5(12):4152–7.
[4] Spentzos D, Levine DA, Ramoni MF, Joseph M, Gu X, Boyd J, et al. Gene expression signature with independent prognostic significance in epithelial ovarian cancer. J Clin Oncol 2004;22(23):4700–10.
[5] Tsuda H, Ito YM, Ohashi Y, Wong KK, Hashiguchi Y, Welch WR, et al. Identification of overexpression and amplification of ABCF2 in clear cell ovarian adenocarcinomas by cDNA microarray analyses. Clin Cancer Res 2005;11(19 Pt 1):6880–8.
[6] Spentzos D, Levine DA, Kolia S, Otu H, Boyd J, Libermann TA, et al. Unique gene expression profile based on pathologic response in epithelial ovarian cancer. J Clin Oncol 2005;23(31):7911–8.
[7] Birrer MJ, Johnson ME, Hao K, Wong KK, Park DC, Bell A, et al. Whole genome oligonucleotide-based array comparative genomic hybridization analysis identified fibroblast growth factor 1 as a prognostic marker for advanced-stage serous ovarian adenocarcinomas. J Clin Oncol 2007;25(16):2281–7.
[8] Takano M, Kikuchi Y, Yaegashi N, Kuzuya K, Ueki M, Tsuda H, et al. Clear cell carcinoma of the ovary: a retrospective multicentre experience of 254 patients with complete surgical staging. Br J Cancer 2006;94(10):1369–74.
[9] Hess V, A'Hern R, Nasiri N, King DM, Blake PR, Barton DP, et al. Mucinous epithelial ovarian cancer: a separate entity requiring specific treatment. J Clin Oncol 2004;22(6):1040–4.
[10] Arnold N, Hagele L, Walz L, Schempp W, Pfisterer J, Bauknecht T, et al. Overrepresentation of 3q and 8q material and loss of 18q material are recurrent findings in advanced human ovarian cancer. Genes Chromosom Cancer 1996;16(1):46–54.
[11] Mayr D, Kanitz V, Anderegg B, Luthardt B, Engel J, Lohrs U, et al. Analysis of gene amplification and prognostic markers in ovarian cancer using comparative genomic hybridization for microarrays and immunohistochemical analysis for tissue microarrays. Am J Clin Pathol 2006;126(1):101–9.
[12] Israeli O, Gotlieb WH, Friedman E, Korach J, Goldman B, Zeltser A, et al. Genomic analyses of primary and metastatic serous epithelial ovarian cancer. Cancer Genet Cytogenet 2004;154(1):16–21.
[13] Schipf A, Mayr D, Kirchner T, Diebold J. Molecular genetic aberrations of ovarian and uterine carcinosarcomas—a CGH and FISH study. Virchows Arch 2008;452(3):259–68.
[14] Kaneda H, Arao T, Tanaka K, Tamura D, Aomatsu K, Kudo K, et al. FOXQ1 is overexpressed in colorectal cancer and enhances tumorigenicity and tumor growth. Cancer Res;70(5):2053–2063.

[15] Matsumoto K, Arao T, Tanaka K, Kaneda H, Kudo K, Fujita Y, et al. mTOR signal and hypoxia-inducible factor-1 alpha regulate CD133 expression in cancer cells. Cancer Res 2009;69(18):7160–4.
[16] Tanaka K, Arao T, Maegawa M, Matsumoto K, Kaneda H, Kudo K, et al. SRPX2 is overexpressed in gastric cancer and promotes cellular migration and adhesion. Int J Cancer 2009;124(5):1072–80.
[17] Iwabuchi H, Sakamoto M, Sakunaga H, Ma YY, Carcangiu ML, Pinkel D, et al. Genetic analysis of benign, low-grade, and high-grade ovarian tumors. Cancer Res 1995;55(24):6172–80.
[18] Sonoda G, Palazzo J, du Manoir S, Godwin AK, Feder M, Yakushiji M, et al. Comparative genomic hybridization detects frequent overrepresentation of chromosomal material from 3q26, 8q24, and 20q13 in human ovarian carcinomas. Genes Chromosom Cancer 1997;20(4):320–8.
[19] Tanner MM, Grenman S, Koul A, Johannsson O, Meltzer P, Pejovic T, et al. Frequent amplification of chromosomal region 20q12-q13 in ovarian cancer. Clin Cancer Res 2000;6(5):1833–9.
[20] Hu J, Khanna V, Jones MW, Surti U. Comparative study of primary and recurrent ovarian serous carcinomas: comparative genomic hybridization analysis with a potential application for prognosis. Gynecol Oncol 2003;89(3):369–75.
[21] Srivastava RK, Srivastave AR, Cho-Chung YS. Synergistic effects of 8-Cl-cAMP and retinoic acids in the inhibition of growth and induction of apoptosis in ovarian cancer cells: induction of retinoic acid receptor beta. Mol Cell Biochem 2000;204 (1–2):1–9.
[22] Yan L, Herrmann V, Hofer JK, Insel PA. beta-adrenergic receptor/cAMP-mediated signaling and apoptosis of S49 lymphoma cells. Am J Physiol Cell Physiol 2000;279 (5):C1665–74.
[23] Wu EH, Tam BH, Wong YH. Constitutively active alpha subunits of G(q/11) and G (12/13) families inhibit activation of the pro-survival Akt signaling cascade. FEBS J 2006;273(11):2388–98.
[24] Frey UH, Alakus H, Wohlschlaeger J, Schmitz KJ, Winde G, van Calker HG, et al. GNAS1 T393C polymorphism and survival in patients with sporadic colorectal cancer. Clin Cancer Res 2005;11(14):5071–7.
[25] Frey UH, Eisenhardt A, Lummen G, Rubben H, Jockel KH, Schmid KW, et al. The T393C polymorphism of the G alpha s gene (GNAS1) is a novel prognostic marker in bladder cancer. Cancer Epidemiol Biomarkers Prev 2005;14(4): 871–7.
[26] Frey UH, Lummen G, Jager T, Jockel KH, Schmid KW, Rubben H, et al. The GNAS1 T393C polymorphism predicts survival in patients with clear cell renal cell carcinoma. Clin Cancer Res 2006;12(3 Pt 1):759–63.
[27] Frey UH, Nuckel H, Sellmann L, Siemer D, Kuppers R, Durig J, et al. The GNAS1 T393C polymorphism is associated with disease progression and survival in chronic lymphocytic leukemia. Clin Cancer Res 2006;12(19):5686–92.

Clinical Cancer Research

# Impact of Serum Hepatocyte Growth Factor on Treatment Response to Epidermal Growth Factor Receptor Tyrosine Kinase Inhibitors in Patients with Non–Small Cell Lung Adenocarcinoma

Kazuo Kasahara[1], Tokuzo Arao[2], Kazuko Sakai[2], Kazuko Matsumoto[2], Asao Sakai[1], Hideharu Kimura[1], Takashi Sone[1], Atsushi Horiike[4], Makoto Nishio[4], Tatsuo Ohira[5], Norihiko Ikeda[5], Takeharu Yamanaka[6], Nagahiro Saijo[3], and Kazuto Nishio[2]

## Abstract

**Purpose:** The epidermal growth factor receptor (EGFR) mutation status has emerged as a validated biomarker for predicting the response to treatment with EGFR-tyrosine kinase inhibitors (EGFR-TKI) in patients with non–small cell lung cancer. However, the responses to EGFR-TKIs vary even among patients with EGFR mutations. We studied several other independently active biomarkers for EGFR-TKI treatment.

**Experimental Design:** We retrospectively analyzed the serum concentrations of 13 molecules in a cohort of 95 patients with non–small cell lung adenocarcinoma who received EGFR-TKI treatment at three centers. The pretreatment serum concentrations of amphiregulin, β-cellulin, EGF, EGFR, epiregulin, fibroblast growth factor-basic, heparin-binding EGF-like growth factor, hepatocyte growth factor (HGF), platelet-derived growth factor β polypeptide, placental growth factor, tenascin C, transforming growth factor-α, and vascular endothelial growth factor (VEGF) were measured using enzyme-linked immunosorbent assay and a multiplex immunoassay system. The associations between clinical outcomes and these molecules were evaluated.

**Results:** The concentrations of HGF and VEGF were significantly higher among patients with progressive disease than among those without progressive disease ($P < 0.0001$). HGF and VEGF were strongly associated with progression-free survival (PFS) and overall survival (OS) in a univariate Cox analysis (all tests for hazard ratio showed $P < 0.0001$). A stratified multivariate Cox model according to EGFR mutation status (mutant, $n = 20$; wild-type, $n = 23$; unknown, $n = 52$) showed that higher HGF levels were significantly associated with a shorter PFS and OS ($P < 0.0001$ for both PFS and OS). These observations were also consistent in the subset analyses.

**Conclusions:** Serum HGF was strongly related to the outcome of EGFR-TKI treatment. Our results suggest that the serum HGF level could be used to refine the selection of patients expected to respond to EGFR-TKI treatment, warranting further prospective study. *Clin Cancer Res; 16(18); 4616–24. ©2010 AACR.*

Selective epidermal growth factor receptor tyrosine kinase inhibitors (EGFR-TKI) block signal transduction pathways implicated in the proliferation and survival of cancer cells (1–3), and show clinical activity against non–small cell lung carcinoma (NSCLC, refs. 4–6). To date, four populations are known to have a better response to EGFR-TKIs: females, never-smokers, adenocarcinoma histology, and patients of East Asian ethnicity (4–6). Active EGFR mutation apparently confers a hyperresponsiveness to gefitinib among NSCLC patients (7, 8). Such mutations affect the ATP-binding cleft of EGFR, and EGFR mutants exhibit constitutive tyrosine kinase activity. Most reported EGFR mutations are either point mutations in exons 18 (G719A/C) and 21 (L858R and L861Q) or in-frame deletions in exon 19 that eliminate five amino acids (ELREA) located at position 745 (9).

A large-scale randomized study, the IRESSA Pan-Asia study (IPASS), comparing gefitinib monotherapy with carboplatin/paclitaxel for 1,217 previously untreated patients with lung adenocarcinoma, was recently completed, and the results showed that the progression-free survival

**Authors' Affiliations:** [1]Respiratory Medicine, School of Medicine, Kanazawa University, Kanazawa, Ishikawa, Japan; [2]Department of Genome Biology, [3]Kinki University School of Medicine, Osaka-Sayama, Osaka, Japan; [4]Thoracic Oncology Center, Cancer Institute Hospital, Japanese Foundation for Cancer Research, and [5]Department of Thoracic Surgery and Oncology, Tokyo Medical University, Tokyo, Japan; and [6]Institute for Clinical Research, National Kyushu Cancer Center, Fukuoka, Japan

**Note:** T. Arao and K. Sakai contributed equally to this work.

**Corresponding Author:** Kazuto Nishio, Department of Genome Biology, Kinki University School of Medicine, 377-2 Ohno-higashi, Osaka-Sayama, Osaka 589-8511, Japan. Phone: 81-72-366-0221 ext. 3150; Fax: 81-72-367-6369; E-mail: knishio@med.kindai.ac.jp.

**doi:** 10.1158/1078-0432.CCR-10-0383

**Translational Relevance**

A high pretreatment serum HGF concentration was strongly associated with poor treatment outcomes, including tumor response, progression-free survival, and overall survival, in patients with non–small cell lung adenocarcinoma treated with epidermal growth factor receptor tyrosine kinase inhibitors (EGFR-TKI). Combined with the EFGR mutation status, measurement of the serum HGF level might further refine the selection of patients likely to respond to EGFR-TKI treatment, especially in the wild-type EGFR subgroup, thereby increasing the clinical benefit of EGFR-TKI treatment.

(PFS) curves of the two arms crossed each other. A subset analysis of the 437 patients whose EGFR mutation status was known revealed that the presence of an EGFR mutation in the tumor was a strong predictor of a better outcome after gefitinib treatment (10). Two recent phase III trials targeting adenocarcinoma patients with EGFR mutations showed that the gefitinib group had a significantly longer PFS than the platinum-doublet therapy group (11, 12). These data indicated EGFR mutation status as a powerful predictor of the tumor response to EGFR-TKIs.

Even among patients with EGFR mutations, however, not all patients respond to EGFR-TKI treatment in like manner; the objective response to EGFR-TKI treatment has remained at 62% to 75% (11–13). In addition, no effective biomarker is currently available for patients with wild-type EGFR tumors (14). These facts motivated us to investigate molecular biomarkers that can be utilized independently of EGFR status to predict the efficacy of EGFR-TKIs. Identifying such a marker would contribute to the further individualization of treatment for NSCLC. In this report, we retrospectively studied the serum concentrations of several molecules in patients with non–small cell lung adenocarcinoma who underwent treatment with EGFR-TKIs.

## Materials and Methods

### Patients

A total of 104 patients with histologically confirmed non–small cell lung adenocarcinoma who had been treated with EGFR-TKIs at three centers (Kanazawa University, Japan; Cancer Institute Hospital, Japan; and Tokyo Medical University, Japan) between 2002 and 2009 were included in this study. Six patients were excluded because their tumor response was not evaluated. A complete clinical data set was not available for three additional patients. Thus, 95 patients were included in the final analysis (Fig. 1A). The tumor response was evaluated every 2 to 3 months using computerized tomography according to the Response Evaluation Criteria in Solid Tumors; the response was then classified as a complete response (CR), a partial response (PR), stable disease (SD), or progressive disease (PD). Clinicopathologic features including age, gender, Eastern Cooperative Oncology Group (ECOG) performance status (PS), tumor-node-metastasis stage, smoking status, and EGFR mutation status were recorded. Direct sequencing of a tumor sample was done to detect active EGFR mutations in 43 patients; 20 of these samples were found to harbor an EGFR mutation (exon 19, $n = 14$; exon 21, $n = 6$), whereas the remaining 23 samples exhibited wild-type EGFR. The mutation status of the other 52 patients was not evaluated. The present study was approved by the institutional review boards of all the centers.

### Preparation of serum samples

Blood samples were collected before the initiation of EGFR-TKI treatment. Separated serum was stocked at -80°C until use.

### Serum HGF levels

Serum HGF concentrations were determined using a Human HGF Quantikine ELISA Kit (R&D Systems) according to the manufacturer's instructions. A 50-μL aliquot of serum per well was examined in duplicate, and the average was used for subsequent analysis. The absorbance of the samples at 450 nm was measured using VERSAmax (Japan Molecular Devices).

### Antibody suspension bead array system

Antibody suspension bead arrays for determining the serum concentrations of 12 molecules were obtained commercially (WideScreen Human Cancer Panel 2, Merck). The markers used in this panel were as follows: amphiregulin, β-cellulin, epidermal growth factor (EGF), EGFR, epiregulin, fibroblast growth factor-basic (FGF-basic), heparin-binding EGF-like growth factor (HB-EGF), platelet-derived growth factor β polypeptide (PDGF-BB), placental growth factor (PlGF), tenascin C (TnC), transforming growth factor α (TGF-α), and vascular endothelial growth factor (VEGF). Data were obtained using a Bio-Plex suspension array system (Bio-Rad Laboratories). The assay was done according to the manufacturer's instructions and a previously described method (15). Serum samples were diluted 1:4 with the appropriate diluents prior to assay. The samples were tested in duplicate, and the averages were used for analysis.

### Statistical analysis

The primary objective was to investigate novel markers correlated with efficacy independently of EGFR-status. If a molecule was very strongly associated with survival after adjustments for the EGFR status and important prognostic factors, then that molecule was deemed as warranting further prospective study to determine whether it is a predictive factor, a prognostic factor, or both.

The distributions of the clinical factors and molecules were compared between patients with PD and those without PD using the Wilcoxon test. In terms of the analysis

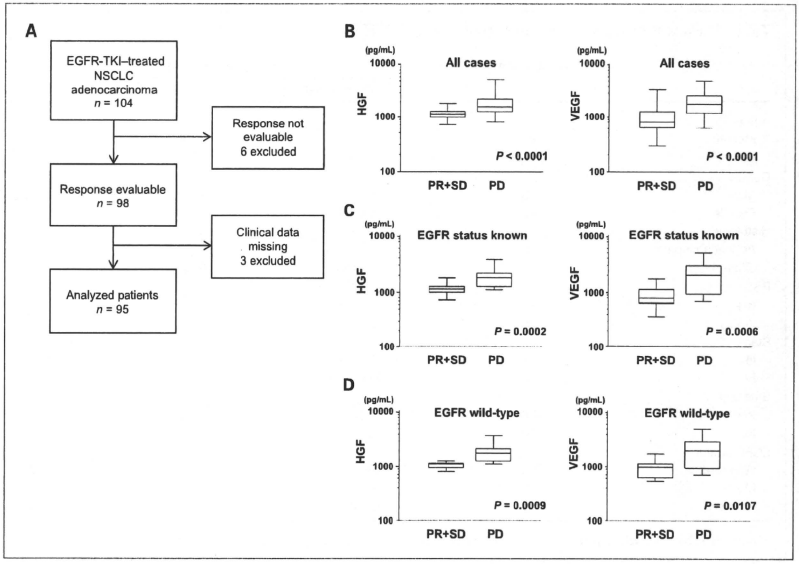


Fig. 1. A, flow diagram of analyzed patients. B to D, box-whisker plots of serum concentrations of HGF (pg/mL) and VEGF (pg/mL) in patients with progressive disease (PD) and those without progressive disease (PR+SD). The plots are drawn for all patients (top; $n = 95$), those with a known EGFR status (middle; $n = 43$), and those with wild-type EGFR (bottom; $n = 23$).

for survival time [PFS and overall survival (OS)], clinical factors including age, gender, ECOG PS, clinical stage, and smoking status were examined using the Cox proportional hazards model. After selecting the important clinical variables, we considered these variables fixedly in a Cox proportional hazards model and then determined which, if any, of the molecules was associated with survival using the backward selection method; thus, any molecules remaining in the final model were significant in a manner that was independent of the important clinical variables at a two-sided level of 0.05 using the Wald test. Log-transformed values were used for the molecules in the Cox models. The proportional hazards assumption was assessed graphically, and an individual time-dependent component was included for each covariate. In the multivariate Cox models, EGFR status (wild-type/mutant/unknown) was treated as a stratified variable. We applied the above analyses to all the cases, to the cases in which the EGFR status was evaluated, and to the cases with wild-type EGFR to check the robustness of the conclusions. The survival curves for PFS and OS were estimated using the Kaplan-Meier method. The Kaplan-Meier curves were shown just to visualize the trends of the association between the molecules and PFS/OS, as any determination of the optimal cutoff point for the molecules relative to the PFS/OS was beyond the scope of the present study. All the statistical analyses were done using SAS for Windows (ver. 9.1.3) and Medcalc for Windows (ver. 11.1.1).

## Results

### Patient results

Of the 95 patients evaluated in this study, all the patients were of Asian ethnicity and had been treated with an EGFR-TKIs (gefitinib, $n = 91$; erlotinib, $n = 4$). Seventy-five (79%) and eight (8%) patients had received prior chemotherapy and radiotherapy, respectively. After the start of EGFR-TKI treatment, a PR was observed in 37 (39%) patients, SD in 25 (26%) patients, and PD in 33 (35%) patients; none of the patients exhibited a CR. The median follow-up period was 29 months. The patient characteristics are shown in Table 1. Regarding tumor response, male gender ($P = 0.0002$), a PS of 2 to 4 ($P = 0.0498$), a positive smoking history ($P = 0.0010$), and a wild-type EGFR status ($P < 0.0001$)

**Table 1.** Patient characteristics and response to EGFR-TKIs

| | Total ($n$ = 95) | Response to EGFR-TKIs | | |
|---|---|---|---|---|
| | | PR+SD ($n$ = 62) | PD ($n$ = 33) | $P$ |
| Age (y) | | | | |
| Median | 64 | 64 | 65 | 0.58 |
| Range | 29-89 | 35-89 | 29-79 | |
| Gender | | | | |
| Male | 53 | 26 (42%) | 27 (82%) | 0.0002 |
| Female | 42 | 36 (58%) | 6 (18%) | |
| Histology | | | | |
| Adenocarcinoma | 95 | 62 (100%) | 33 (100%) | - |
| Other | 0 | 0 (0%) | 0 (0%) | |
| PS | | | | |
| 0-1 | 70 | 50 (81%) | 20 (61%) | 0.0498 |
| 2-4 | 25 | 12 (19%) | 13 (39%) | |
| Stage | | | | |
| III | 11 | 7 (11%) | 4 (12%) | 1.00 |
| IV | 84 | 55 (89%) | 29 (88%) | |
| Smoking | | | | |
| Yes | 56 | 29 (47%) | 27 (82%) | 0.0010 |
| No | 39 | 33 (53%) | 6 (18%) | |
| EGFR status | | | | |
| Wild-type | 23 | 9 (15%) | 14 (42%) | <0.0001* |
| Mutant | 20 | 20 (32%) | 0 (0%) | |
| Unknown | 52 | 33 (53%) | 19 (58%) | |

*Comparison between wild-type and mutant. $P$ values are calculated using the $t$-test for age and Fisher's exact test for other variables.

were significantly less sensitive to EGFR-TKI treatment (Table 1). These results are consistent with those of a previous report (16).

**Serum concentrations of 13 molecules**

We measured the serum concentrations of 13 molecules: amphiregulin, β-cellulin, EGF, EGFR, epiregulin, FGF-basic, HB-EGF, HGF, PDGF-BB, PIGF, TnC, TGF-α, and VEGF. Among them, many samples (>80%) showed a value that could not be measured or that was below the standard range for amphiregulin, β-cellulin, epiregulin, FGF-basic, and TGF-α; these molecules were omitted from subsequent analyses. Therefore, only the correlations between clinical outcome and the serum concentrations of

**Table 2.** Distributions of serum concentrations according to response status to EGFR-TKIs

| | All cases ($n$ = 95) | | | EGFR status known ($n$ = 43) | | | EGFR wild-type ($n$ = 23) | | |
|---|---|---|---|---|---|---|---|---|---|
| | Median | | $P$ | Median | | $P$ | Median | | $P$ |
| | PR+SD | PD | | PR+SD | PD | | PR+SD | PD | |
| EGF | 199.1 | 252.0 | 0.0334 | 235.2 | 268.7 | 0.23 | 252.8 | 268.7 | 0.87 |
| EGFR | 2,100.8 | 2,092.0 | 0.58 | 2,096.0 | 2,030.6 | 0.89 | 2,083.6 | 2,030.6 | 0.97 |
| HB-EGF | 74.6 | 114.8 | 0.0066 | 79.0 | 129.9 | 0.0277 | 71.8 | 129.9 | 0.14 |
| HGF | 1,150.8 | 1,580.0 | <0.0001 | 1,136.5 | 1,810.9 | 0.0002 | 1,116.4 | 1,810.9 | 0.0009 |
| PDGF-BB | 15,574.3 | 14,388.8 | 0.53 | 14,228.0 | 19,031.5 | 0.12 | 13,385.2 | 19,031.5 | 0.11 |
| PIGF | 3.8 | 7.0 | 0.25 | 9.0 | 11.4 | 0.39 | 2.5 | 11.4 | 0.58 |
| TnC | 643.2 | 979.0 | 0.0278 | 557.0 | 1,211.6 | 0.0233 | 614.5 | 1,211.6 | 0.07 |
| VEGF | 808.8 | 1,787.0 | <0.0001 | 800.5 | 2023.0 | 0.0006 | 984.5 | 2023.0 | 0.0107 |

NOTE: Median values of eight serum concentrations are tabulated according to the response status. The Wilcoxon test was used to assess the difference in the median values between PR+SD and PD.

**Table 3.** Univariate analysis of clinical molecular factors for progression-free and overall survival

| | | All cases ($n$ = 95) | | | |
|---|---|---|---|---|---|
| | | Progression-free survival | | Overall survival | |
| | | HR (95% CI) | $P$ | HR (95% CI) | $P$ |
| Age | 65< vs. ≤65 y | 0.93 (0.60-1.43) | 0.74 | 1.22 (0.76-1.96) | 0.42 |
| Gender | Male vs. Female | 1.85 (1.19-2.88) | 0.0061 | 2.36 (1.43-3.88) | 0.0007 |
| PS | 2-4 vs. 0-1 | 1.66 (1.04-2.67) | 0.0356 | 2.55 (1.53-4.25) | 0.0003 |
| Stage | IV vs. III | 0.66 (0.34-1.25) | 0.20 | 1.27 (0.61-2.67) | 0.53 |
| Smoking | Yes vs. No | 1.65 (1.06-2.58) | 0.0270 | 2.19 (1.33-3.62) | 0.0022 |
| EGF | | 1.17 (0.90-1.51) | 0.24 | 1.15 (0.86-1.53) | 0.34 |
| EGFR | | 1.37 (0.68-2.79) | 0.38 | 1.37 (0.62-3.05) | 0.44 |
| HB-EGF | | 1.49 (1.09-2.03) | 0.0116 | 1.55 (1.10-2.18) | 0.0124 |
| HGF | | 10.24 (5.48-19.2) | <0.0001 | 5.57 (3.28-9.46) | <0.0001 |
| PDGF-BB | | 1.11 (0.80-1.54) | 0.53 | 1.16 (0.82-1.65) | 0.39 |
| PlGF | | 1.10 (0.87-1.38) | 0.44 | 1.29 (1.01-1.66) | 0.04 |
| TnC | | 1.74 (1.30-2.34) | 0.0002 | 2.19 (1.56-3.06) | <0.0001 |
| VEGF | | 3.54 (2.33-5.38) | <0.0001 | 3.52 (2.25-5.50) | <0.0001 |

(*Continued on the following page*)

EGF, EGFR, HB-EGF, HGF, PDGF-BB, PlGF, TnC, and VEGF were analyzed.

### Tumor response and serum concentrations

The serum concentrations of EGF, HB-EGF, HGF, TnC, and VEGF were significantly higher among patients with PD than among those without PD (Table 2). Among these molecules, HGF and VEGF exhibited marked differences in tumor response. These results were unchanged when subsets of patients with a known EGFR status ($n$ = 43) as well as patients with wild-type EGFR ($n$ = 23) were analyzed (Fig. 1B-D). These observations suggested that HGF and VEGF were significantly associated with tumor response, independent of the EGFR mutation status. The sensitivity and specificity of HGF and VEGF for discriminating PD from PR plus SD were determined using the cutoff values according to a previously reported methodology (17). The cutoff values for HGF and VEGF for discriminating PD from PR plus SD were 1,228 pg/mL and 1,187 pg/mL, respectively. The sensitivity and specificity of HGF for discriminating PD from PR plus SD were 0.848 and 0.677, and those for VEGF were 0.788 and 0.710, respectively.

### Univariate analysis of clinical molecular factors for PFS and OS

The numbers of observed events were 85 cases for PFS and 70 cases for OS. The median PFS and OS were 4.0 and 8.9 months, respectively. Among the clinical factors that were examined, a male gender, a poor PS, and a positive smoking history were significantly related with a poor PFS and OS (Table 3). Regarding the serum concentrations of the molecules, higher concentrations of HGF, HB-EGF, TnC, and VEGF were significantly associated with a shorter PFS and OS (Table 3). Similar to the results for tumor response, HGF and VEGF were associated with both PFS and OS when all the cases were analyzed, with all tests exhibiting a hazard ratio (HR) with a $P$ value <0.0001. Similar results were obtained when subsets of patients with a known EGFR status and patients with wild-type EGFR were analyzed (data not shown). Figure 2 shows the Kaplan-Meier estimates for PFS and OS with regard to the concentrations of serum HGF and VEGF. Although a determination of the optimal cutoff values was beyond the scope of this study, all the patients were divided into one of four groups according to the quartile values for each molecule. The curves provided a clear trend indicating that the outcomes became poorer as the concentrations of these molecules increased. To compare these results with those for patients with a known EGFR status in Table 3, we calculated the univariate HRs for the EGFR status (wild-type versus mutant) in the subset of patients with a known EGFR status. These HRs were 3.49 [95% confidence interval (95% CI), 1.76-6.92; $P$ = 0.0004] and 3.32 (95% CI, 1.52-7.24; $P$ = 0.0026) for PFS and OS, respectively.

### Multivariate analysis stratified according to EGFR mutation status for PFS and OS

The purpose of this study was to investigate novel markers correlated with the response to EGFR-TKI treatment independently of the EGFR status. However, the EGFR status (wild-type/mutant/unknown) did not satisfy the assumption of proportional hazards in our data. Hence, we adopted a stratified model, and the multivariate Cox analyses always included the EGFR status as a stratification factor when estimating the adjusted HRs (ref. 18; Table 4). Gender and PS remained statistically significant at a level

**Table 3.** Univariate analysis of clinical molecular factors for progression-free and overall survival (Cont'd)

| EGFR status known ($n$ = 43) | | | |
|---|---|---|---|
| **Progression-free survival** | | **Overall survival** | |
| **HR (95% CI)** | ***P*** | **HR (95% CI)** | ***P*** |
| 0.73 (0.36-1.47) | 0.37 | 1.01 (0.47-2.16) | 0.99 |
| 1.86 (0.94-3.69) | 0.07 | 1.78 (0.84-3.76) | 0.13 |
| 1.59 (0.74-3.44) | 0.2365 | 2.90 (1.26-6.66) | 0.0123 |
| 0.66 (0.25-1.72) | 0.39 | 1.85 (0.55-6.15) | 0.32 |
| 2.38 (1.17-4.87) | 0.0174 | 3.01 (1.31-6.93) | 0.0096 |
| 1.22 (0.75-1.98) | 0.42 | 1.46 (0.79-2.69) | 0.23 |
| 1.25 (0.52-2.98) | 0.62 | 1.38 (0.50-3.83) | 0.54 |
| 1.30 (0.81-2.07) | 0.277 | 1.64 (0.89-3.01) | 0.11 |
| 11.71 (3.78-36.3) | <0.0001 | 18.17 (4.93-67.0) | <0.0001 |
| 1.22 (0.79-1.89) | 0.38 | 1.58 (0.84-2.99) | 0.16 |
| 1.21 (0.87-1.68) | 0.25 | 1.34 (0.92-1.96) | 0.12 |
| 1.55 (1.05-2.28) | 0.0275 | 1.89 (1.21-2.96) | 0.0055 |
| 3.03 (1.63-5.62) | 0.0005 | 3.19 (1.65-6.17) | 0.0006 |

NOTE: Univariate analysis was done for all the patients and in a subset of patients with a known EGFR mutation status. Log-transformed values are used for all the molecules.

of 0.05 in a multivariate model that included the three clinical variables with a small $P$ value (<0.20) in a univariate analysis. Smoking status was no longer significant ($P$ = 0.46 and $P$ = 0.40 for PFS and OS, respectively) because it was highly correlated with gender ($P < 0.0001$, Fisher's exact test). Thus, we fixed gender and PS in the Cox model and identified significant molecules by backward selection with $P \geq 0.05$ as a removal criterion. Table 4 shows the final

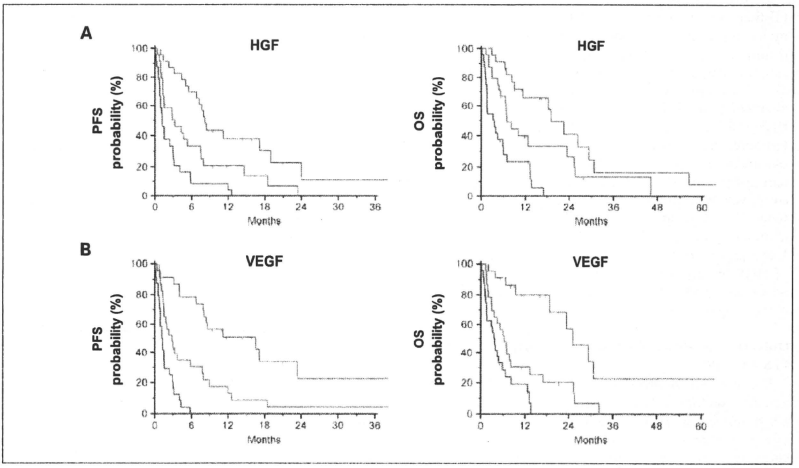


Fig. 2. Kaplan-Meier curves for PFS and OS. Patients were divided into four groups according to the quartile values of each molecule. For HGF (A), red group, patients with <1,061 pg/mL; yellow, with 1,061 to 1,231 pg/mL; green, with 1,232 to 1,521 pg/mL; blue, with >1,522 pg/mL. For VEGF (B), red group, patients with <700 pg/mL; yellow, with 700 to 1,115 pg/mL; green, with 1,116 to 1,769 pg/mL; blue, with >1,769 pg/mL.

**Table 4.** Final multivariate model for progression-free survival and overall survival

| | | Progression-free survival | | Overall survival | |
|---|---|---|---|---|---|
| | | HR (95% CI) | P | HR (95% CI) | P |
| Gender | Male vs. Female | 1.29 (0.76-2.20) | 0.34 | 1.92 (1.06-3.47) | 0.0303 |
| PS | 2-4 vs. 0-1 | 0.61 (0.34-1.09) | 0.10 | 1.55 (0.87-2.75) | 0.14 |
| HGF | | 6.31 (2.60-15.3) | <0.0001 | 4.01 (2.20-7.32) | <0.0001 |
| VEGF | | 2.01 (1.14-3.57) | 0.0165 | | |

NOTE: Gender and PS are fixed in the model. Molecular markers were then selected using the backward selection procedure with a removal probability of 0.05. In all the steps, a Cox model stratified according to the EGFR status (wild-type/mutant/unknown) was applied. Log-transformed values are used for all the molecules.

model using this procedure. HGF (HR, 6.31; 95% CI, 2.60-15.3; $P < 0.0001$) and VEGF (HR, 2.01; 95% CI, 1.14-3.57; $P = 0.0165$) were significant for PFS, whereas only HGF (HR, 4.01; 95% CI, 2.20-7.32; $P < 0.0001$) was significant for OS; a high concentration of HGF showed a shorter PFS and OS independently of the clinical variables of EGFR status, gender, and PS (Table 4). In the final model, no interaction was shown between the EGFR status and HGF ($P = 0.84$ and $P = 0.20$ for PFS and OS, respectively). The results shown in Table 4 were also stable in analyses of subsets of patients with a known EGFR status as well as patients with wild-type EGFR (data not shown).

## Discussion

HGF was identified as a natural ligand of the MET receptor and belongs to the plasminogen family (19). It contains a hairpin loop followed by four kringle domains flanked by an activation portion and a serine protease domain devoid of proteolytic activity (20). In cancer cells, activation of the Met receptor increases invasion and metastasis, and allows the survival of cancer cells in the bloodstream in the absence of anchorage (20). In addition, HGF is well known as a potent angiogenic cytokine, and Met activation can modify the microenvironment to facilitate cancer progression (21). Therefore, HGF-MET signaling is regarded as an oncogenic signaling pathway, and intensive therapeutic approaches focusing on this signaling pathway are ongoing in the field of cancer treatment (22).

Meanwhile, a high serum HGF concentration has been associated with a poor prognosis in many malignant neoplastic diseases, including colorectal, esophageal, gastric, and prostate cancer, as well as malignant myeloma (23–25). Where cancer treatment is concerned, high peripheral and portal HGF serum levels are related to a poor prognosis after hepatic resection in hepatocellular carcinoma (HCC) patients (26). The HGF level is also elevated in patients with myeloma, and patients with higher HGF levels tend to have a poorer prognosis; furthermore, treatment with high-dose chemotherapy reduced the serum HGF level in the majority of these patients (27). The above-mentioned evidence suggests that a high serum HGF level is a relatively well-established predictor of poor prognosis. Ishikawa et al. have shown that, besides HGF, amphiregulin and TGF-α are predictors of a poor response to gefitinib in EGFR status-unknown advanced non–small cell lung cancer (17). Although we did not obtain similar results, these molecules are expected to be noninvasive predictive biomarkers.

On the other hand, few reports have examined the predictive value of HGF with regard to the clinical outcomes of chemotherapy or molecular-targeting drugs. A recent study showed that the pretreatment HGF concentrations in the peripheral blood plasma as well as in the bone marrow plasma of patients who achieved a complete or very good partial response were significantly lower than those in patients who had a partial or worse response (28). In this study, we showed, for the first time, that a high pretreatment serum HGF level was associated with poor clinical outcomes, including tumor response and survival time, in patients treated with EGFR-TKIs. The robust association of this parameter with outcome regardless of the EGFR mutation status clearly suggests that the serum HGF level could be useful for predicting the response to EGFR-TKI treatment on an individual basis. The direct sequencing for EGFR mutations could have produced false-negative results, presenting a bias for the relevance of HGF in patients with supposed wild-type EGFR. We plan to evaluate EGFR mutations using a highly sensitive detection method in a future study.

Although we do not have any definitive biological data to address the question of why a high pretreatment serum HGF level is associated with a poor clinical outcome after EGFR-TKI treatment, several studies are worth noting. Engelman et al. showed that the amplification of MET causes gefitinib resistance by driving the ERBB3 (HER3)-dependent activation of phosphoinositide 3-kinase, and they proposed that MET amplification may promote drug resistance in other ERBB-driven cancers (29). Yano et al. clearly showed that HGF-mediated MET activation is involved in gefitinib resistance in lung adenocarcinoma with EGFR-activating mutations (30). In addition, a recent study has clearly shown that HGF accelerates the development of MET amplification both *in vitro* and *in vivo*, mediating the EGFR kinase inhibitor

resistance caused by either MET amplification or autocrine HGF production (31). These studies indicate that the activation of HGF-MET signaling confers resistance to EGFR-TKIs. Therefore, lung cancer cells producing high amounts of HGF might mediate drug resistance to EGFR-TKIs, leading to poor treatment outcomes.

In this study, a multivariate analysis revealed that the serum HGF level was independently associated with a poor treatment outcome. This finding indicates the possibility of using the serum HGF level to refine the indications for patients who are likely to respond to EGFR-TKI treatment. In particular, patients with wild-type EGFR are considered to be less sensitive to EGFR-TKIs, but our results might allow the identification of a selective subgroup of these patients who might actually benefit from this treatment. When used in combination with EGFR mutation status, the serum HGF level might increase the clinical benefit of EGFR-TKIs by allowing the further individualization of this treatment. We plan to conduct a prospective study to validate the ability of the serum HGF level to predict the response to EGFR-TKI treatment.

## Disclosure of Potential Conflicts of Interest

No potential conflicts of interest were disclosed.


## Acknowledgments

We thank Ms. Tomoko Kitayama for technical assistance.

## Grant Support

Third-Term Comprehensive 10-Year Strategy for Cancer Control, a Grant-in-Aid for Scientific Research, the Program for the Promotion of Fundamental Studies in Health Sciences of the National Institute of Biomedical Innovation (NiBio), a Grant-in-Aid for Cancer Research (H20-20-9) from the Ministry of Health, Labour and Welfare and a Grant-in-Aid for Scientific Research from the Ministry of Education, Culture, Sports, Science and Technology of Japan (19209018).

The costs of publication of this article were defrayed in part by the payment of page charges. This article must therefore be hereby marked *advertisement* in accordance with 18 U.S.C. Section 1734 solely to indicate this fact.

Received 02/16/2010; revised 06/29/2010; accepted 07/11/2010; published OnlineFirst 08/02/2010.


## References


1. Ciardiello F, Caputo R, Tortora G, et al. Antitumor effect and potentiation of cytotoxic drugs activity in human cancer cells by ZD-1839 (Iressa), an epidermal growth factor receptor-selective tyrosine kinase inhibitor. Clin Cancer Res 2000;6:2053–63.
2. Moasser MM, Basso A, Averbuch SD, Rosen N. The tyrosine kinase inhibitor ZD1839 (Iressa) inhibits HER2-driven signaling and suppresses the growth of HER2-overexpressing tumor cells. Cancer Res 2001;61:7184–8.
3. Koizumi F, Kanzawa F, Nishio K, et al. Synergistic interaction between the EGFR tyrosine kinase inhibitor gefitinib (Iressa) and the DNA topoisomerase I inhibitor CPT-11 (irinotecan) in human colorectal cancer cells. Int J Cancer 2004;108:464–72.
4. Thatcher N, Chang A, Parikh P, et al. Gefitinib plus best supportive care in previously treated patients with refractory advanced non-small-cell lung cancer: results from a randomised, placebo-controlled, multicentre study (Iressa Survival Evaluation in Lung Cancer). Lancet 2005;366:1527–37.
5. Shepherd FA, Rodrigues Pereira J, Ciuleanu T, et al. Erlotinib in previously treated non-small-cell lung cancer. N Engl J Med 2005;353:123–32.
6. Fukuoka M, Yano S, Giaccone G, et al. Multi-institutional randomized phase II trial of gefitinib for previously treated patients with advanced non-small-cell lung cancer (The IDEAL 1 Trial). J Clin Oncol 2003;21:2237–46.
7. Lynch TJ, Bell DW, Sordella R, et al. Activating mutations in the epidermal growth factor receptor underlying responsiveness of non-small-cell lung cancer to gefitinib. N Engl J Med 2004;350:2129–39.
8. Paez JG, Janne PA, Lee JC, et al. EGFR mutations in lung cancer: correlation with clinical response to gefitinib therapy. Science 2004;304:1497–500.
9. John T, Liu G, Tsao MS. Overview of molecular testing in non-small-cell lung cancer: mutational analysis, gene copy number, protein expression and other biomarkers of EGFR for the prediction of response to tyrosine kinase inhibitors. Oncogene 2009 Suppl 1:S14–23.
10. Mok TS, Wu YL, Thongprasert S, et al. Gefitinib or carboplatin-paclitaxel in pulmonary adenocarcinoma. N Engl J Med 2009;361:947–57.
11. Mitsudomi T, Morita S, Yatabe Y, et al, for the West Japan Oncology Group. Gefitinib versus cisplatin plus docetaxel in patients with non-small-cell lung cancer harbouring mutations of the epidermal growth factor receptor (WJTOG3405): an open label, randomised phase 3 trial. Lancet Oncol 2010;11:121–8.
12. Maemondo M, Inoue A, Kobayashi K, et al. Gefitinib or chemotherapy for non-small-cell lung cancer with mutated EGFR. N Engl J Med 2010;362:2380–8.
13. Tamura K, Okamoto I, Kashii T, et al, West Japan Thoracic Oncology Group. Multicentre prospective phase II trial of gefitinib for advanced non-small cell lung cancer with epidermal growth factor receptor mutations: results of the West Japan Thoracic Oncology Group trial (WJTOG0403). Br J Cancer 2008;98:907–14.
14. Laurent-Puig P, Lievre A, Blons H. Mutations and response to epidermal growth factor receptor inhibitors. Clin Cancer Res 2009;15:1133–9.
15. Kimura H, Kasahara K, Sekijima M, Tamura T, Nishio K. Plasma MIP-1β levels and skin toxicity in Japanese non-small cell lung cancer patients treated with the EGFR-targeted tyrosine kinase inhibitor, gefitinib. Lung Cancer 2005;50:393–9.
16. Miller VA, Kris MG, Shah N, et al. Bronchioloalveolar pathologic subtype and smoking history predict sensitivity to gefitinib in advanced non-small-cell lung cancer. J Clin Oncol 2004;22:1103–9.
17. Ishikawa N, Daigo Y, Takano A, et al. Increases of amphiregulin and transforming growth factor-α in serum as predictors of poor response to gefitinib among patients with advanced non-small cell lung cancers. Cancer Res 2005;65:9176–84.
18. Kleinbaum DG, Klein M. Survival analysis: a self-learning text. New York: Springer; 2005. p. 173–210.
19. Naldini L, Vigna E, Narsimhan RP, et al. Hepatocyte growth factor (HGF) stimulates the tyrosine kinase activity of the receptor encoded by the proto-oncogene c-MET. Oncogene 1991;6:501–4.
20. Benvenuti S, Comoglio PM. The MET receptor tyrosine kinase in invasion and metastasis. J Cell Physiol 2007;213:316–25.
21. Gentile A, Trusolino L, Comoglio PM. The Met tyrosine kinase receptor in development and cancer. Cancer Metastasis Rev 2008;27:85–94.
22. Eder JP, Vande Woude GF, Boerner SA, LoRusso PM. Novel therapeutic inhibitors of the c-Met signaling pathway in cancer. Clin Cancer Res 2009;15:2207–14.
23. Toiyama Y, Miki C, Inoue Y, Okugawa Y, Tanaka K, Kusunoki M. Serum hepatocyte growth factor as a prognostic marker for stage II or III colorectal cancer patients. Int J Cancer 2009;125:1657–62.
24. Ren Y, Cao B, Law S, et al. Hepatocyte growth factor promotes

cancer cell migration and angiogenic factors expression: a prognostic marker of human esophageal squamous cell carcinomas. Clin Cancer Res 2005;11:6190–7.

25. Tanaka K, Miki C, Wakuda R, Kobayashi M, Tonouchi H, Kusunoki M. Circulating level of hepatocyte growth factor as a useful tumor marker in patients with early-stage gastric carcinoma. Scand J Gastroenterol 2004;39:754–60.
26. Chau GY, Lui WY, Chi CW, et al. Significance of serum hepatocyte growth factor levels in patients with hepatocellular carcinoma undergoing hepatic resection. Eur J Surg Oncol 2008;34:333–8.
27. Seidel C, Lenhoff S, Brabrand S, et al, Nordic Myeloma Study Group. Hepatocyte growth factor in myeloma patients treated with high-dose chemotherapy. Br J Haematol 2002;119:672–6.
28. Pour L, Svachova H, Adam Z, et al. Pretreatment hepatocyte growth factor and thrombospondin-1 levels predict response to high-dose chemotherapy for multiple myeloma. Neoplasma 2010;57:29–34.
29. Engelman JA, Zejnullahu K, Mitsudomi T, et al. MET amplification leads to gefitinib resistance in lung cancer by activating ERBB3 signaling. Science 2007;316:1039–43.
30. Yano S, Wang W, Li Q, et al. Hepatocyte growth factor induces gefitinib resistance of lung adenocarcinoma with epidermal growth factor receptor-activating mutations. Cancer Res 2008;68:9479–87.
31. Turke AB, Zejnullahu K, Wu YL, et al. Preexistence and clonal selection of MET amplification in EGFR mutant NSCLC. Cancer Cell 2010;17:77–88.

Cancer Science
The official journal of the Japanese Cancer Association JCA

# Role of ZNF143 in tumor growth through transcriptional regulation of DNA replication and cell-cycle-associated genes

Hiroto Izumi,[1] Tetsuro Wakasugi,[2] Shohei Shimajiri,[3] Akihide Tanimoto,[4] Yasuyuki Sasaguri,[3] Eiji Kashiwagi,[1] Yoshihiro Yasuniwa,[1] Masaki Akiyama,[1] Bin Han,[1] Ying Wu,[1] Takeshi Uchiumi,[5] Tokuzo Arao,[6] Kazuto Nishio,[6] Ryuta Yamazaki[7] and Kimitoshi Kohno[1,8]

Departments of [1]Molecular Biology, [2]Otorhinolaryngology and [3]Pathology and Cell Biology, School of Medicine, University of Occupational and Environmental Health, Kitakyushu; [4]Department of Tumor Pathology, Field of Oncology, Kagoshima University Graduate School of Medical and Dental Sciences, Kagoshima; [5]Department of Clinical Chemistry and Laboratory Medicine, Graduate School of Medical Sciences, Kyushu University, Fukuoka; [6]Department of Genome Biology, Kinki University School of Medicine, Osaka-Sayama, Osaka; [7]Yakult Central Institute for Microbiological Research, Tokyo, Japan

(Received July 12, 2010 Revised August 13, 2010 Accepted August 16, 2010 Accepted manuscript online August 20, 2010)

**The cell cycle is strictly regulated by numerous mechanisms to ensure cell division. The transcriptional regulation of cell-cycle-related genes is poorly understood, with the exception of the E2F family that governs the cell cycle. Here, we show that a transcription factor, zinc finger protein 143 (ZNF143), positively regulates many cell-cycle-associated genes and is highly expressed in multiple solid tumors. RNA-interference (RNAi)-mediated knockdown of ZNF143 showed that expression of 152 genes was downregulated in human prostate cancer PC3 cells. Among these ZNF143 targets, 41 genes (27%) were associated with cell cycle and DNA replication including cell division cycle 6 homolog (CDC6), polo-like kinase 1 (PLK1) and minichromosome maintenance complex component (MCM) DNA replication proteins. Furthermore, RNAi of ZNF143 induced apoptosis following G2/M cell cycle arrest. Cell growth of 10 lung cancer cell lines was significantly correlated with cellular expression of ZNF143. Our data suggest that ZNF143 might be a master regulator of the cell cycle. Our findings also indicate that ZNF143 is a member of the growing list of non-oncogenes that are promising cancer drug targets. (*Cancer Sci*, doi: 10.1111/j.1349-7006.2010.01725.x, 2010)**

Transcriptional regulation of gene expression requires the orchestrated recruitment of transcription factors by sequence-specific DNA binding regulators. Staf was initially identified as the transcriptional activator of the RNA polymerase III-dependent *Xenopus* tRNA gene.[1] It has recently been shown that its human ortholog zinc finger protein 143 (ZNF143; formerly known as hStaf) is also involved in RNA-polymerase-II-dependent gene transcription.[2,3] The DNA binding domain of ZNF143 is located in the central part of the protein and consists of seven zinc finger domains.[1,4] The ZNF143 DNA binding site is thought to be at least 18 bp long because the protein has seven zinc fingers; by analogy, the well-known zinc finger transcription factor Sp family and members of the KLF family contain three zinc fingers and recognize DNA sequences approximately 6 bp long.[5] Recently, it has been shown by a bioinformatics approach that ZNF143 binding sites are widely distributed in the CpG island-type promoters of the human genome.[6] Functional classification of ZNF143 target genes has revealed that many of the identified genes are important for cell growth: 27% of the genes are categorized as cell cycle/DNA replication/DNA repair proteins.

We have previously reported that expression of ZNF143 is induced by DNA-damaging agents and is enhanced in cisplatin-resistant cell lines.[7] ZNF143 binds preferentially to cisplatin-modified DNA. We also found that ZNF143 binding sites are frequently found in the promoter region of DNA repair genes.

Here, we investigated the ZNF143 target genes by RNA interference (RNAi). One hundred and fifty-two genes were downregulated by ZNF143-specific small interfering RNA (siRNA) transfection. Among them, 41 genes are categorized as concerned with cell cycle and DNA replication. ZNF143 was highly expressed in cancer cells when compared with non-tumor regions. Downregulation of ZNF143 effectively induced G2/M cell cycle arrest and apoptosis, indicating that ZNF143 might be a promising molecular target for anti-cancer drugs.

## Materials and Methods

**Cell culture and antibodies.** Human prostate cancer cells PC3,[7] human cervical cancer cells HeLa[7] and human bladder cancer cells T24[8] were cultured in minimum essential medium (MEM). Human colon cancer cells Caco-2[9] and DLD1,[10] human glioblastoma CCF-STTG1[11] and human astrocytoma cells U343[11] were cultured in Dulbecco's modified Eagle's minimal essential medium. Human lung cancer cells A549,[12] B203L,[12] PC9,[12] A110L,[12] QG56,[12] SQ1,[12] B1203L,[12] PC10,[12] 904L[12] and A529L[12] were cultured in RPMI 1640 medium. These media were purchased from Nissui Seiyaku (Tokyo, Japan) and contained 10% fetal bovine serum. Cell lines were maintained in a 5% $CO_2$ atmosphere at 37°C. Antibodies against peroxiredoxin 4 (PRDX4) (sc-23974), minichromosome maintenance complex component 2 (MCM2) (sc-9839), MCM3 (sc-9850), MCM4 (sc-28317), MCM5 (sc-22780) and MCM6 (sc-9843) were purchased from Santa Cruz Biotechnology (Santa Cruz, CA, USA). Antibodies against Flag (M2) and β-actin (A5441) were purchased from Sigma Aldrich (St Louis, MO, USA). Antibodies against aurora B kinase (AURKB) (1788-1) and nuclear factor (erythroid-derived 2)-like 2 (Nrf2) (2073-1) were purchased from Epitomics (Burlingame, CA, USA). Antibodies against PLK1 (37-7000) and CDC6 (05-550) were purchased from Invitrogen (Carlsbad, CA, USA) and Upstate Biotech (Lake Placid, NY, USA), respectively. The polyclonal antibody against the high mobility group B2 (HMGB2) was described previously.[13] The polyclonal antibody against ZNF143 was raised by multiple immunizations of a New Zealand white rabbit with synthetic peptides. The synthetic peptide sequences were MLLAQINRDSQGMTEFPGGGMEAQHVTLC and QLGEQPSLEEAIRIASRIQQGETPGLDD for ZNF143.

[8]To whom correspondence should be addressed.
E-mail: k-kohno@med.uoeh-u.ac.jp

doi: 10.1111/j.1349-7006.2010.01725.x

**Plasmid construction.** To prepare luciferase (luc) reporter plasmids, genomic DNA was amplified with the following primer pairs: CDC6 luc1, 5′-AGATCTCGCCTCCCAGCGTGCTTTG-CGG-3′ and 5′-AAGCTTCACCCAGCTCCGCTGCCTCAC-3′; CDC6 luc2, 5′-AGATCTACTACGCCTCCCAGCGTGCTTTG-CGG-3′ and 5′-AAGCTTCACCCAGCTCCGCTGCCTCAC-3′; PLK1 luc, 5′-AGATCTCCGCATCCACGCCGGGTTTGG-3′ and 5′-AAGCTTGCGCTGCAGACCTCGATCCGAGC-3′; AURKB luc, 5′-AGATCTCACTGGGGGAATTTGGGGAAAC-3′ and 5′-AAGCTTGGGGTCCAAGGCACTGCTACTC-3′; MCM2 luc, 5′-AGATCTCGAACTCCTGAGCTTGTGATCC-3′ and 5′-AAGCTTCTCCGCCACTACAGCAACAACC-3′; and HMGB2 luc, 5′-AGATCTGGGCGGCGCACGGGAGACCC-3′ and 5′-AAGCTTCCCGCAGAGCGGCCGGACCC-3′. Restriction enzyme sites are underlined. These PCR products were cloned and ligated into the *Bgl*II-*Hind*III site of the pGL3-basic vector (Promega, Madison, WI, USA). The pGL3-P2 (promoter vector) containing an SV40 promoter upstream of the luciferase gene was purchased from Promega. Preparation of 3xFlag-ZNF143 expression plasmid was described previously.[7]

**Knockdown with siRNA.** The following double-stranded RNA 25-bp oligonucleotides were commercially generated (Invitrogen): *ZNF143* siRNA, *siZNF #1*, 5′-GCTGGAAGATGGTA-CCACAGCTTAT-3′ (sense) and 5′-ATAAGCTGTGGTACC-ATCTTCCAGC-3′ (antisense); and *siZNF #2*, 5′-GGACGAC-GTTGTTTCTACACAAGTA-3′ (sense) and 5′-TACTTGTGT-AGAAACAACGTCGTCC-3′ (antisense). Two hundred picomoles of siRNA were mixed with 10 μL Lipofectamine 2000 (Qiagen, Hilden, Germany) according to the manufacturer's instructions. After 20 min, $1 \times 10^6$ cancer cells were gently mixed and incubated for a further 20 min. Transfected cells were used for oligonucleotide microarray study, cell proliferation assays, flow cytometry and western blotting.

**Oligonucleotide microarray study and microarray analysis.** A microarray procedure was performed as described previously.[14] In brief, total RNA extracts were collected from PC3 cells transfected with ZNF143 #2 siRNA or control siRNA in duplicate, as described above. Eight GeneChips (Affymetrix, Santa Clara, CA, USA) were used for analysis. The microarray analysis was performed using the BRB Array Tools software ver. 3.3.0 (http://linus.nci.nih.gov/BRB-ArrayTools.html) developed by Dr Richard Simon and Amy Peng.

**Cell proliferation assays.** The cell proliferation assay was described previously.[15] Briefly, siRNA-transfected cancer cells were seeded into 12-well plates at a density of $5 \times 10^4$ cells per well. Twenty-four hours after transfection was set as time zero. The cells were harvested by trypsinization and counted every 24 h with a Coulter-type cell size analyzer (CDA-500; Sysmex Corp., Kobe, Japan).

**Flow cytometry.** Flow cytometry was described previously.[15] Briefly, siRNA-transfected PC3 cells ($1 \times 10^6$) were seeded into 90-mm plates. After 72 h, the cells were analyzed using an EpicsXL-MCL flow cytometer (Beckman-Coulter, Miami, FL, USA). For assessment of apoptosis, an Annexin V-fluorescein isothiocyanate (FITC) Apoptosis Detection kit II (BD Biosciences, San Jose, CA, USA) was used.

**Western blotting.** Transfection of expression plasmid and preparation of nuclear proteins was described previously.[7] ZNF143 expression plasmid- or siRNA-transfected PC3 cells were collected after 48–72 h and nuclear protein or whole cell lysate was subjected to western blotting. Detection was performed using enhanced chemiluminescence (Amersham, Piscataway, NJ, USA). The protein expression levels were quantitated using a Multi Gauge Version 3.0 (Fujifilm, Tokyo, Japan).

**Chromatin immunoprecipitation (ChIP) assays.** The cloning of PC3 cells stably expressing 3xFlag-tagged ZNF143 has been described previously.[7] Purified DNA from these cells was used for PCR analysis with the indicated primer pairs (Table S1). The PCR products were separated by electrophoresis on 2% agarose gels and were stained with ethidium bromide.

**Reporter assays.** One $\times 10^5$ PC3 cells per well were seeded into 12-well plates. The following day, 1 μg luciferase reporter plasmid was transfected with 30 pmol *ZNF143* siRNA or control siRNA using 5 μL Lipofectamine 2000 (Qiagen). After 48 h, luciferase activity was detected using a Picagene kit (Toyo Ink, Tokyo, Japan). Light intensity was measured using a luminometer (Luminescencer JNII RAB-2300; Atto, Japan). The results shown are normalized for protein concentration measured using the Bradford method, and are representative of at least three independent experiments.

**Human tissue samples.** Samples were obtained from the surgical pathology archive of the Department of Pathology and Cell Biology of The University of Occupational and Environmental Health in Kitakyushu, Japan. The selected tissues consisted of one surgically resected case each of esophageal carcinoma, gastric adenocarcinoma, squamous cell carcinoma of the lung, urothelial carcinoma of the urinary bladder, testicular seminoma and cerebral astrocytoma. These cases were classified according to the World Health Organization Histological Typing of each tissue. The diagnosis was re-evaluated and confirmed by at least three board-certified surgical pathologists who had examined formalin-fixed, paraffin-embedded tissue sections stained with hematoxylin and eosin or other appropriate immunohistochemical stains.

**Immunohistochemistry.** The specimens were fixed in 20% formaldehyde and embedded in paraffin. Four micrometer-thick tissue sections were deparaffinized, dehydrated with graded xylene and alcohol, and incubated in 3% hydrogen peroxide for 5 min at room temperature to eliminate endogenous peroxidase activity. Antigen retrieval for the anti-ZNF143 antibody was performed with 0.1 M citrate buffer (pH 6.0) in an autoclave for 15 min. The sections were then incubated with anti-ZNF143 antibody (dilution ratio 1:200). The Envision plus system (Dako, Carpinteria, CA, USA) was used for antibody-bridge labeling, with hematoxylin counterstaining.

**Statistical analysis.** Pearson's correlation was used for statistical analysis, and significance was set at the 5% level.

## Results

***ZNF143* expression is required for cancer cell growth.** We estimated specificity of both ZNF143 antibody and *ZNF143* siRNA. ZNF143-specific antibody recognized both endogenous 90 kDa protein and exogenous 3xFlag-ZNF143 protein (Fig. 1A). Endogenous ZNF143 protein was completely abolished with treatment of specific siRNA against ZNF143 (Fig. 1B). An *in silico* genome-wide screen for ZNF143 binding sites suggested that many of the target genes are involved in cell growth.[6] To confirm these results, we first investigated whether *ZNF143* expression is required for cancer cell growth. At first, downregulation of *ZNF143* expression effectively reduced cell growth in PC3 cells (Fig. 2A). Analysis of cell cycle profiles was performed on human prostate cancer PC3 cells after transfection with two different *ZNF143*-specific siRNA. A marked increase in G2/M phase cells was observed when cells were transfected with *ZNF143* siRNA (Fig. 2B,C). In addition, knockdown of *ZNF143* expression induced apoptosis, as shown by an increased percentage of cells in the subG1 population (~5%), whereas only 1% of cells treated with control siRNA was in the subG1 population (Fig. 2C). To extend these results, the cells were stained with an anti-Annexin V-FITC antibody. Treatment with control siRNA did not induce apoptosis, whereas knockdown of *ZNF143* expression resulted in an increase in the percentage of annexin V positive cells (Fig. 2D).



doi: 10.1111/j.1349-7006.2010.01725.x

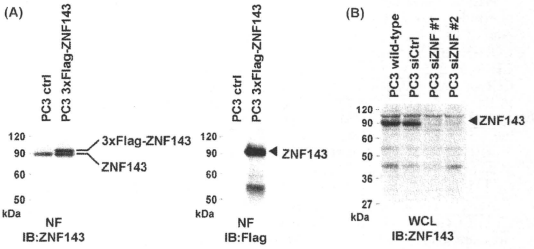


**Fig. 1.** Specificity of anti-zinc finger protein 143 (ZNF143) antibody and *ZNF143* small interfering RNA (siRNA). (A) PC3 cells were transfected with or without 3xFlag-ZNF143 and nuclear proteins (50 μg) were used for western blotting with anti-ZNF143 and anti-Flag antibodies. (B) PC3 cells were transfected with or without *ZNF143* siRNA and whole cell lysate (100 μg) were used for western blotting with anti-ZNF143 antibody. siZNF #1 and #2 indicate *ZNF143* siRNA #1 and #2, respectively.

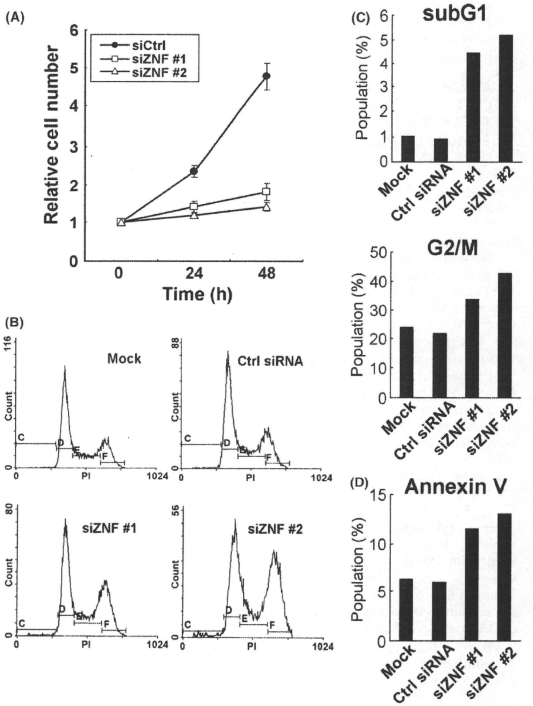


**Fig. 2.** Knockdown of *ZNF143* induces G2/M arrest. (A) PC3 cells were transfected with control siRNA (siCtrl), *ZNF143* siRNA #1 (siZNF #1) or *ZNF143* siRNA #2 (siZNF #2). Cells were counted after the indicated times, with time zero being 24 h after transfection. The results were normalized to cell numbers at time zero. The points represent the mean of at least three independent experiments; the bars show the SD. (B) PC3 cells were transfected with or without the indicated siRNA. Cells were harvested after 72 h and used for propidium iodide (PI) staining. DNA content in single cells was measured. siZNF #1 and #2 indicate *ZNF143* siRNAs #1 and #2, respectively. (C) SubG1 and G2/M populations were calculated from the results of part (B). (D) siRNA-transfected PC3 cells were stained with Annexin-V-fluorescein isothiocyanate and PI, and the percentage of apoptotic cells (annexin V positive and PI negative) was determined by flow cytometry. siZNF #1 and #2 indicate *ZNF143* siRNA #1 and #2, respectively.

**DNA microarray analysis with *ZNF143*-specific siRNA.** We then evaluated global expression profiles to determine the real ZNF143 target genes by cDNA microarray. One hundred and fifty-two genes were downregulated <0.4-fold after *ZNF143*-specific siRNA transfection, whereas 84 genes were upregulated more than 2.5-fold after downregulation of *ZNF143* expression (Table S2). To categorize the 152 downregulated genes, we used the Database for Annotation, Visualization and Integrated Discovery (DAVID) Bioinformatics Resources Program (http://david.abcc.ncifcrf.gov/). Among 152 genes, 41 (27.0%) were categorized as concerned with the cell cycle/DNA replication (Table 1). Next, we searched for putative ZNF143

**Table 1. Cell cycle/DNA replication associated genes downregulated following zinc finger protein 143 (ZNF143) knockdown**

| Gene ID | Symbol | Accession | Gene name | Fold change† |
|---|---|---|---|---|
| 23397 | NCAPH | NM_015341 | Barren homolog 1 (Drosophila) | 0.174 |
| 991 | CDC20 | NM_001255 | CDC20 cell division cycle 20 homolog (*Saccharomyces cerevisiae*) | 0.221 |
| 57405 | SPC25 | NM_020675 | Spindle pole body component 25 homolog (*S. cerevisiae*) | 0.234 |
| 4174 | MCM5 | NM_006739 | MCM5 minichromosome maintenance deficient 5, cell division cycle 46 (*S. cerevisiae*) | 0.234 |
| 9212 | AURKB | NM_004217 | Aurora kinase B | 0.239 |
| 890 | CCNA2 | NM_001237 | Cyclin A2 | 0.248 |
| 990 | CDC6 | NM_001254 | CDC6 cell division cycle 6 homolog (*S. cerevisiae*) | 0.252 |
| 4173 | MCM4 | NM_005914 | MCM4 minichromosome maintenance deficient 4 (*S. cerevisiae*) | 0.256 |
| 4176 | MCM7 | NM_005916 | MCM7 minichromosome maintenance deficient 7 (*S. cerevisiae*) | 0.258 |
| 5347 | PLK1 | NM_005030 | Polo-like kinase 1 (Drosophila) | 0.266 |
| 7465 | WEE1 | NM_003390 | WEE1 homolog (*Schizosaccharomyces pombe*) | 0.278 |
| 81620 | CDT1 | NM_030928 | DNA replication factor | 0.284 |
| 83461 | CDCA3 | NM_031299 | Cell division cycle associated 3 | 0.288 |
| 5888 | RAD51 | NM_002875 | RAD51 homolog (RECA homolog, *Escherichia coli*) (*S. cerevisiae*) | 0.289 |
| 4171 | MCM2 | NM_004526 | MCM2 minichromosome maintenance deficient 2, mitotin (*S. cerevisiae*) | 0.289 |
| 56992 | KIF15 | NM_020242 | Kinesin family member 15 | 0.290 |
| 3148 | HMGB2 | NM_002129 | High-mobility group box 2 | 0.295 |
| 113130 | CDCA5 | NM_080668 | Cell division cycle associated 5 | 0.301 |
| 54443 | ANLN | NM_018685 | Anillin, actin binding protein (Scraps homolog, Drosophila) | 0.320 |
| 55388 | MCM10 | NM_018518 | MCM10 minichromosome maintenance deficient 10 (*S. cerevisiae*) | 0.332 |
| 4172 | MCM3 | NM_002388 | MCM3 minichromosome maintenance deficient 3 (*S. cerevisiae*) | 0.334 |
| 9918 | NCAPD2 | NM_014865 | Chromosome condensation-related SMC-associated protein 1 | 0.336 |
| 11004 | KIF2C | NM_006845 | Kinesin family member 2C | 0.348 |
| 1017 | CDK2 | NM_001798 | Cyclin-dependent kinase 2 | 0.348 |
| 51512 | GTSE1 | NM_016426 | G-2 and S-phase expressed 1 | 0.353 |
| 9088 | PKMYT1 | NM_004203 | Protein kinase, membrane associated tyrosine/threonine 1 | 0.356 |
| 5984 | RFC4 | NM_002916 | Replication factor C (Activator 1) 4, 37KDA | 0.357 |
| 3835 | KIF22 | NM_007317 | Kinesin family member 22 | 0.358 |
| 10403 | NDC80 | NM_006101 | Kinetochore associated 2 | 0.359 |
| 699 | BUB1 | NM_004336 | BUB1 budding uninhibited by benzimidazoles 1 homolog (Yeast) | 0.360 |
| 9055 | PRC1 | NM_003981 | Protein regulator of cytokinesis 1 | 0.363 |
| 9700 | ESPL1 | NM_012291 | Extra spindle poles like 1 (*S. cerevisiae*) | 0.365 |
| 55143 | CDCA8 | NM_018101 | Cell division cycle associated 8 | 0.369 |
| 1104 | RCC1 | NM_001269 | Regulator of chromosome condensation 1 | 0.376 |
| 5982 | RFC2 | NM_002914 | Replication factor C (Activator 1) 2, 40KDA | 0.376 |
| 9787 | DLG7 | NM_014750 | Discs, large homolog 7 (Drosophila) | 0.391 |
| 10051 | SMC4 | NM_005496 | SMC4 structural maintenance of chromosomes 4-like 1 (Yeast) | 0.391 |
| 9493 | KIF23 | NM_004856 | Kinesin family member 23 | 0.397 |
| 4751 | NEK2 | NM_002497 | NIMA (never in mitosis gene A)-related kinase 2 | 0.399 |
| 899 | CCNF | NM_001761 | Cyclin F | 0.399 |
| 22974 | TPX2 | NM_012112 | TPX2, microtubule-associated, homolog (*Xenopus laevis*) | 0.399 |

List of cell cycle/DNA-replication-associated genes with fold change marked <0.4. †Fold change indicates the average of expression data of ZNF143 siRNA/control siRNA.

binding sites in the promoter region of these genes. All 41 genes had at least one ZNF143 binding site within 1 kb of the putative transcription start site (Table 1).

**Validation of the ZNF143 target genes.** To validate the microarray expression data, we performed western blotting, ChIP assays and reporter assays. We obtained eight specific antibodies for proteins among the 41 cell cycle/DNA replication regulators with ZNF143 binding site(s). As shown in Figure 3, the expression of nine proteins was decreased by *ZNF143* siRNA transfection. In particular, PLK1, CDC6 and HMGB2 were substantially decreased, whereas β-actin and PRDX4, which do not have a ZNF143 binding site, were not affected by *ZNF143* siRNA transfection. Next, we examined whether ZNF143 directly regulates the expression of these genes using ChIP and luciferase reporter assays. For ChIP assays, we used stable transfectants that expressed three flag tags at the N-terminus of ZNF143.[7] As shown in Figure 4A, ZNF143 bound to the promoters of the seven genes that contained a ZNF143 binding site. The promoter region of *PRDX4*, which does not have a ZNF143 binding site, was used as a negative control. We also investigated the luciferase reporter activities of five genes. The promoter activities of *CDC6*, *PLK1*, *AURKB*, *MCM2* and *HMGB2* were clearly decreased by transfection with *ZNF143*-specific siRNA #2 (Fig. 4B). Myslinski *et al.*[6] reported that 58% of genes that had a ZNF143 binding site contained the submotif ACTACN in their 5′ regions, and that their promoter activities were higher than those of promoters that lacked the submotif. To confirm these results, we prepared two CDC6 promoters: CDC6 luc2 contained the ACTACN sequence and CDC6 luc1 did not. As shown in Figure 4C, our results were consistent with the findings of Myslinski *et al.*, and *ZNF143* siRNA reduced both CDC6 promoter activities, with or without the ACTACN motif, in the same ratio (Fig. 4B).

**Correlation between ZNF143 expression and cell growth in human lung cancer.** ZNF143 regulates the gene expressions



doi: 10.1111/j.1349-7006.2010.01725.x

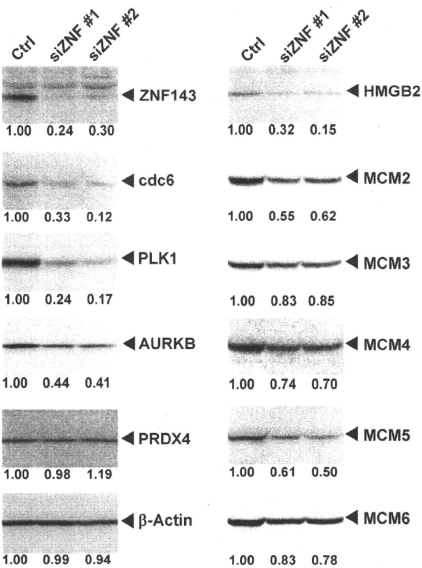


**Fig. 3.** *ZNF143* small interfering RNA (siRNA) reduced the expression of cell cycle/DNA replication-related genes. siRNA-transfected PC3 cells were used for western blotting. Quantitation of protein expression levels is shown under the panels. siZNF #1 and #2 indicate *ZNF143* siRNA #1 and #2, respectively.

associated with the cell cycle and DNA replication. We investigated the cellular expression level of ZNF143 and doubling time with 10 lung cancer cell lines. ZNF143 expression was different in each cancer cell line as compared with Nrf2 and inversely correlated with doubling time (Fig. 5A,B). This result is consistent with repression of cell growth by downregulation of ZNF143 in lung cell cancer A549 and 904L (Fig. 5C). Repression of cell growth by downregulation of ZNF143 was also observed in HeLa, DLD1, Caco-2, T24, CCF-STTG1 and U343 (data not shown).

**ZNF143 expression in human cancer specimens.** To investigate further whether highly proliferative cancer cells are characterized by increased ZNF143 expression, tissue sections of surgical specimens from cancer patients were analyzed by immunohistochemistry (Fig. 6). Six solid tumors (esophageal carcinoma, gastric adenocarcinoma, squamous cell carcinoma of the lung, urothelial carcinoma of the urinary bladder, testicular seminoma and cerebral astrocytoma) were analyzed in comparison with adjacent non-tumor samples. Nuclear-localized ZNF143 was strongly expressed in cancer cells. Expression of ZNF143 was low or weak in non-tumor tissue.

## Discussion

We have identified a number of genes that are induced by treatment with anti-cancer agents and/or overexpressed in drug-resistant cells.[7,14,16–24] The drug sensitivity of cancer cells is governed by the complex pathways involved in the pathogenesis of cancer,[25,26] and identification of the molecules governing cancer cell growth is emerging as a primary theme of molecular therapies. The transcription factor ZNF143 is stress-inducible and overexpressed in cisplatin-resistant cells.[7,27] We found ZNF143 binding sites in the promoter region of many DNA repair genes and propose that ZNF143 regulates the expression of DNA repair genes. It has been shown recently that ZNF143 binding sites are widely distributed in the human genome and are located in the promoters of approximately 1000 human genes.[6] This suggests that ZNF143 might regulate basic cellular functions at the transcriptional level.

Many studies have indicated that the cellular content of cell-cycle-related gene products is strictly regulated post-translationally by the ubiquitin–proteasome system.[28,29] On the other hand, little is known about the transcriptional regulation of cell-cycle-related genes. The E2F family of transcription factors is well known to be a master regulator of cell proliferation and is regulated by the retinoblastoma tumor suppressor gene.[30] In this report, downregulation of ZNF143 strongly induced G2/M arrest. On the contrary, downregulation of E2F induced G1 cell cycle arrest, indicating that the role of ZNF143 may be quite distinct from that of E2F in the cell cycle. ZNF143 target genes have been identified by a combination of *in silico* and experimental approaches.[6] Myslinski *et al.*[6] used eleven 18-bp binding sites in a genome-wide motif search and identified approximately 1000 genes as ZNF143 target genes. Functional classification of these genes indicated that the majority of the identified genes are important for cell growth. Consistently, our results clearly showed that ZNF143 is required for cancer cell growth (Figs 2,5). RNAi-mediated knockdown of ZNF143 showed that the expression of 152 genes was downregulated in human prostate cancer PC3 cells (Table S1). Among these, 41 genes are categorized as concerned with cell cycle/DNA replication (Table 1). The human genome database suggests that approximately 500–600 genes are assigned for cell cycle/DNA replication. Based on our data, approximately 7.5% (41 genes/500–600 genes) of cell cycle/DNA replication genes might be directly or indirectly regulated by ZNF143. On the other hand, ZNF143 regulates only approximately 0.5% (110 genes/23 000–27 000 genes) of other genes except for cell cycle/DNA replication. It is noteworthy that important cell-cycle-associated kinases such as *PLK1*, *AURKB*, *WEE1*, budding uninhibited by benzimidazoles (*BUB1*) and cyclin-dependent kinase 2 (*CDK2*) are target genes for ZNF143. Only nine (*SPC25, CDC6, PLK1, RAD51, MCM3, KIF2C, GTSE1, ESPL1, CDCA8*) (22%) of 41 genes were present in the ZNF143 target gene list identified by the *in silico* genome screen.[6] We also found putative ZNF143 binding sites in many DNA repair genes;[7] however, only four (*Rad51, BRCA1, FEN1, EXO1*) genes were downregulated by ZNF143 siRNA. It has been shown that BUB family expression is required for cancer cell growth but not for normal cells, indicating that the BUB family is one of the genes involved in non-oncogene addiction.[31,32] It is an interesting finding that BUB1 and BUB1B[33] are target genes of ZNF143. These indicate that ZNF143 specifically regulates genes associated with cell cycle/DNA replication and is one of the master regulators of DNA metabolism including cell cycle and cell growth.

It is well established that transcription factors do not make good targets for drug design, because transcription factors form multiple complexes with other cofactors. Our immunohistochemical studies have shown that ZNF143 is highly expressed in cancer cells (Fig. 6). RNAi-mediated knockdown of *ZNF143* induced apoptosis following G2/M cell cycle arrest (Fig. 2). Because cell-cycle-associated kinases have a critical role in cell cycle progression, these kinases comprise a promising set of targets

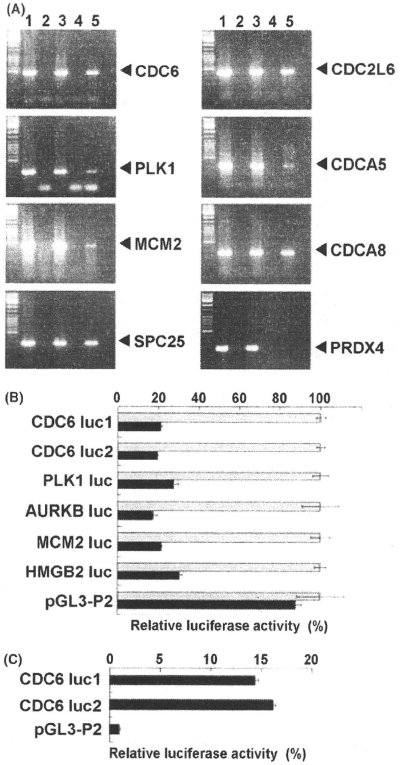


Fig. 4. Luciferase reporter and chromatin immunoprecipitation assays. (A) Soluble chromatin was prepared from flag tagged zinc finger protein 143 (ZNF143) stable transfectants (lanes 3–5) or mock transfectants (lanes 1 and 2), and immunoprecipitated with anti-mouse IgG (lane 4) or anti-Flag (M2) antibodies (lanes 2 and 5). Extracted immunoprecipitated DNA (lanes 2, 4 and 5) and soluble chromatin (lanes 1 and 3) were amplified using specific primer pairs for the indicated promoter regions. The PCR products for *CDC6, PLK1, MCM2, SPC25, CDC2L6, CDCA5, CDCA8* and *PRDX4* were 463, 296, 423, 258, 411, 342, 260 and 153 bp, respectively. (B) PC3 cells were transfected with reporter plasmid and *ZNF143* small interfering RNA (siRNA). Luciferase activities were normalized to each reporter activity with control siRNA. The gray and black bars indicate control siRNA and *ZNF143* siRNA #2, respectively. Bars represent ± SD. (C) PC3 cells were transfected with reporter plasmid. The results were normalized to the protein concentration and are representative of at least three independent experiments. Both CDC6 luc1 and luc2 have a ZNF143 binding site, and CDC6 luc2 also has the ACTACN motif in the ZNF143 binding sequence. Luciferase activities were normalized to the empty vector pGL3-P2. Bars represent ± SD.

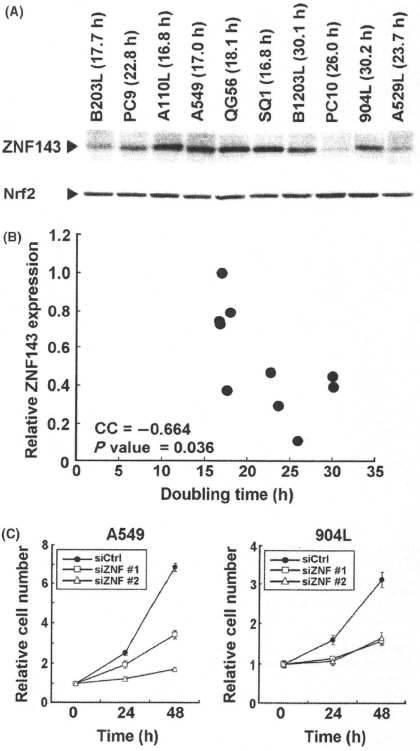


Fig. 5. Correlation between zinc finger protein 143 (ZNF143) expression and cell growth. (A) Nuclear protein (50 μg) was used for western blotting with anti-ZNF143 and anti-Nrf2 antibodies. The doubling time for each cell lines is also shown. (B) Expression of ZNF143 and Nrf2 were quantitated using a Multi Gauge Version 3.0. using Figure 5A, and ZNF143 expression was normalized by Nrf2. The maximum expression levels of ZNF143 were set to 100. CC, coefficient of correlation. (C) A549 and 904L cells were transfected with control siRNA (siCtrl), *ZNF143* siRNA #1 (siZNF #1) or *ZNF143* siRNA #2 (siZNF #2). The cell proliferation assay is described in Figure 2A.

for anti-cancer drugs.[34,35] Among the ZNF143 target cell-cycle-associated kinases, both PLK1 and AURKB are overexpressed in many types of cancer.[36–39] Our data showed that RNAi-mediated knockdown of *ZNF143* effectively downregulated the expression of both PLK1 and AURKB (Fig. 3). The MCM proteins are required for pre-replication complex formation, DNA replication initiation and DNA synthesis. It is well known that the MCM proteins are highly expressed in human cancers. Therefore, the MCM proteins are diagnostic markers and promising targets for anti-cancer drug development.[40] As shown in Figure 3, several MCM proteins are targets of ZNF143. Because ZNF143 regulates the expression of both DNA replication and cell cycle regulatory members, ZNF143 may be a promising target for cancer diagnostics and therapies.



doi: 10.1111/j.1349-7006.2010.01725.x

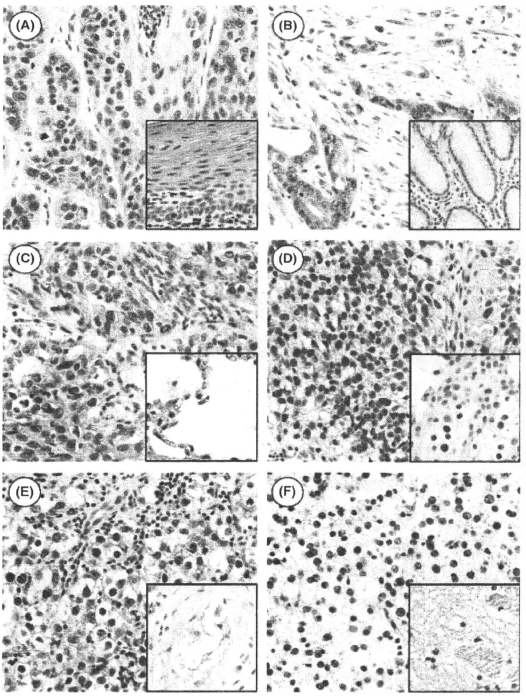


**Fig. 6.** Immunohistochemical analysis of zinc finger protein 143 (ZNF143) expression in various human tumor tissues. Nuclear expression of the ZNF143 protein was seen in all cancer cells, while low or weak nuclear expression was seen in normal adjacent tissues (inset). The selected tissues consisted of surgically resected cases of esophageal carcinoma (A), gastric adenocarcinoma (B), squamous cell carcinoma of the lung (C), urothelial carcinoma of the urinary bladder (D), testicular seminoma (E) and cerebral astrocytoma (F).

We found Ets binding sites in the promoter region of the ZNF143 gene. The Ets family is one of the largest families of transcription factors and is known to be involved in diverse cellular functions. The Ets family is a proto-oncogene and highly expressed in various cancers,[41] indicating that ZNF143 expression might be regulated by the Ets family. Therefore, further studies to investigate the correlation between Ets and ZNF143 expression with clinicopathological data should help in understanding the role of ZNF143 in cancer.

## Acknowledgments

This study was supported by Grants-in-Aid for Scientific Research from the Ministry for Education, Culture, Sports, Science and Technology of Japan (17016075), University of Occupational and Environmental Health (UOEH) Japan, Grant for Advanced Research and the Vehicle Racing Commemorative Foundation. K. Kohno received a research grant from Yakult Co., Ltd., Tokyo, Japan. The authors thank Ms H. Isagai for her technical assistance.

## Disclosure Statement

R. Yamazaki is an employee of Yakult Central Institute for Microbiological Research, Tokyo, Japan.

## References

1 Myslinski E, Krol A, Carbon P. ZNF76 and ZNF143 are two human homologs of the transcriptional activator Staf. *J Biol Chem* 1998; **273**: 21998–2006.
2 Schaub M, Myslinski E, Schuster C, Krol A, Carbon P. Staf, a promiscuous activator for enhanced transcription by RNA polymerase II and III. *EMBO J* 1997; **16**: 173–81.
3 Rincon JC, Engler SK, Hargrove BW, Kunkel GR. Molecular cloning of a cDNA encoding human SPH-binding factor, a conserved protein that binds to the enhancer-like region of the U6 small nuclear RNA gene promoter. *Nucleic Acids Res* 1998; **26**: 4846–52.
4 Schaub M, Krol A, Carbon P. Structural organization of Staf-DNA complexes. *Nucleic Acids Res* 2000; **28**: 2114–21.
5 Kubota H, Yokota S, Yanagi H, Yura T. Transcriptional regulation of the mouse cytosolic chaperonin subunit gene Cctα/t-complex polypeptide 1 by selenocysteine tRNA gene transcription activating factor family zinc finger proteins. *J Biol Chem* 2000; **275**: 28641–8.
6 Myslinski E, Gérard MA, Krol A, Carbon P. A genome scale location analysis of human Staf/ZNF143-binding sites suggests a widespread role for

human Staf/ZNF143 in mammalian promoters. *J Biol Chem* 2006; **281**: 39953–62.
7 Wakasugi T, Izumi H, Uchiumi T *et al.* ZNF143 interacts with p73 and is involved in cisplatin resistance through the transcriptional regulation of DNA repair genes. *Oncogene* 2007; **26**: 5194–203.
8 Takano H, Ise T, Nomoto M *et al.* Structural and functional analysis of the control region of the human DNA topoisomerase II alpha gene in drug-resistant cells. *Anticancer Drug Des* 1999; **14**: 87–92.
9 Torigoe T, Izumi H, Wakasugi T *et al.* DNA topoisomerase II poison TAS-103 transactivates GC-box-dependent transcription via acetylation of Sp1. *J Biol Chem* 2005; **280**: 1179–85.
10 Minagawa N, Nakayama Y, Inoue Y *et al.* 4-[3,5-Bis(trimethylsilyl) benzamido] benzoic acid inhibits angiogenesis in colon cancer through reduced expression of vascular endothelial growth factor. *Oncol Res* 2004; **14**: 407–14.
11 Abe T, Mori T, Kohno K *et al.* Expression of 72 kDa type IV collagenase and invasion activity of human glioma cells. *Clin Exp Metastasis* 1994; **12**: 296–304.
12 Tanabe M, Izumi H, Ise T *et al.* Activating transcription factor 4 increases the cisplatin resistance of human cancer cell lines. *Cancer Res* 2003; **63**: 8592–5.
13 Imamura T, Izumi H, Nagatani G *et al.* Interaction with p53 enhances binding of cisplatin-modified DNA by high mobility group 1 protein. *J Biol Chem* 2001; **276**: 7534–40.
14 Igarashi T, Izumi H, Uchiumi T *et al.* Clock and ATF4 transcription system regulates drug resistance in human cancer cell lines. *Oncogene* 2007; **26**: 4749–60.
15 Takahashi M, Shimajiri S, Izumi H *et al.* Y-box binding protein-1 is a novel molecular target for tumor vessels. *Cancer Sci* 2010; **101**: 1367–73.
16 Kidani A, Izumi H, Yoshida Y *et al.* Thioredoxin2 enhances the damaged DNA binding activity of mtTFA through direct interaction. *Int J Oncol* 2009; **35**: 1435–40.
17 Yokomizo A, Ono M, Nanri H *et al.* Cellular levels of thioredoxin associated with drug sensitivity to cisplatin, mitomycin C, doxorubicin, and etoposide. *Cancer Res* 1995; **55**: 4293–6.
18 Ohga T, Koike K, Ono M *et al.* Role of the human Y box-binding protein YB-1 in cellular sensitivity to the DNA-damaging agents cisplatin, mitomycin C, and ultraviolet light. *Cancer Res* 1996; **56**: 4224–8.
19 Ise T, Izumi H, Nagatani G *et al.* Structural characterization of the human interleukin-13 receptor alpha1 gene promoter. *Biochem Biophys Res Commun* 1999; **265**: 387–94.
20 Kato K, Nomoto M, Izumi H *et al.* Structure and functional analysis of the human STAT3 gene promoter: alteration of chromatin structure as a possible mechanism for the upregulation in cisplatin-resistant cells. *Biochim Biophys Acta* 2000; **1493**: 91–100.
21 Nagatani G, Nomoto M, Takano H *et al.* Transcriptional activation of the human HMG1 gene in cisplatin-resistant human cancer cells. *Cancer Res* 2001; **61**: 1592–7.
22 Murakami T, Shibuya I, Ise T *et al.* Elevated expression of vacuolar proton pump genes and cellular PH in cisplatin resistance. *Int J Cancer* 2001; **93**: 869–74.
23 Shiota M, Izumi H, Onitsuka T *et al.* Twist promotes tumor cell growth through YB-1 expression. *Cancer Res* 2008; **68**: 98–105.
24 Miyamoto N, Izumi H, Noguchi T *et al.* Tip60 is regulated by circadian transcription factor clock and is involved in cisplatin resistance. *J Biol Chem* 2008; **283**: 18218–26.
25 Torigoe T, Izumi H, Ishiguchi H *et al.* Cisplatin resistance and transcription factors. *Curr Med Chem Anticancer Agents* 2005; **5**: 15–27.
26 Kohno K, Uchiumi T, Niina I *et al.* Transcription factors and drug resistance. *Eur J Cancer* 2005; **41**: 2577–86.
27 Ishiguchi H, Izumi H, Torigoe T *et al.* ZNF143 activates gene expression in response to DNA damage and binds to cisplatin-modified DNA. *Int J Cancer* 2004; **111**: 900–9.
28 Nalepa G, Rolfe M, Harper JW. Drug discovery in the ubiquitin-proteasome system. *Nat Rev Drug Discov* 2006; **5**: 596–613.
29 Huang L, Chen CH. Proteasome regulators: activators and inhibitors. *Curr Med Chem* 2009; **16**: 931–9.
30 Chen HZ, Tsai SY, Leone G. Emerging roles of E2Fs in cancer: an exit from cell cycle control. *Nat Rev Cancer* 2009; **9**: 785–97.
31 Malumbres M, Barbacid M. Cell cycle kinases in cancer. *Curr Opin Genet Dev* 2007; **17**: 60–5.
32 Schlabach MR, Luo J, Solimini NL *et al.* Cancer proliferation gene discovery through functional genomics. *Science* 2008; **319**: 620–4.
33 Myslinski E, Gérard MA, Krol A, Carbon P. Transcription of the human cell cycle regulated BUB1B gene requires hStaf/ZNF143. *Nucleic Acids Res* 2007; **35**: 3453–64.
34 Lapenna S, Giordano A. Cell cycle kinases as therapeutic targets for cancer. *Nat Rev Drug Discov* 2009; **8**: 547–66.
35 de Cárcer G, Pérez de Castro I, Malumbres M. Targeting cell cycle kinases for cancer therapy. *Curr Med Chem* 2007; **14**: 969–85.
36 Strebhardt K, Ullrich A. Targeting polo-like kinase 1 for cancer therapy. *Nat Rev Cancer* 2006; **6**: 321–30.
37 Takai N, Hamanaka R, Yoshimatsu J, Miyakawa I. Polo-like kinases (Plks) and cancer. *Oncogene* 2005; **24**: 287–91.
38 Gautschi O, Heighway J, Mack PC, Purnell PR, Lara PN Jr, Gandara DR. Aurora kinases as anticancer drug targets. *Clin Cancer Res* 2008; **14**: 1639–48.
39 Mountzios G, Terpos E, Dimopoulos MA. Aurora kinases as targets for cancer therapy. *Cancer Treat Rev* 2008; **34**: 175–82.
40 Lei M. The MCM complex: its role in DNA replication and implications for cancer therapy. *Curr Cancer Drug Targets* 2005; **5**: 365–80.
41 Tsantoulis PK, Gorgoulis VG. Involvement of E2F transcription factor family in cancer. *Eur J Cancer* 2005; **41**: 2403–14.

## Supporting Information

Additional Supporting Information may be found in the online version of this article:

**Table S1.** Primer pairs used for Chromatin immunoprecipitation (ChIP) assays.

**Table S2.** The list of selected genes with fold change marked >2.5 or <0.4.

Please note: Wiley-Blackwell are not responsible for the content or functionality of any supporting materials supplied by the authors. Any queries (other than missing material) should be directed to the corresponding author for the article.



doi: 10.1111/j.1349-7006.2010.01725.x

Published OnlineFirst December 3, 2010; DOI:10.1158/1078-0432.CCR-09-2755

Clinical Cancer Research

*Cancer Therapy: Preclinical*

# Antitumor Activity of BIBF 1120, a Triple Angiokinase Inhibitor, and Use of VEGFR2$^+$pTyr$^+$ Peripheral Blood Leukocytes as a Pharmacodynamic Biomarker *In Vivo*

Kanae Kudo[1,2], Tokuzo Arao[1], Kaoru Tanaka[1], Tomoyuki Nagai[1], Kazuyuki Furuta[1], Kazuko Sakai[1], Hiroyasu Kaneda[1], Kazuko Matsumoto[1], Daisuke Tamura[1], Keiichi Aomatsu[1], Marco A. De Velasco[1], Yoshihiko Fujita[1], Nagahiro Saijo[3], Masatoshi Kudo[2], and Kazuto Nishio[1]

## Abstract

**Purpose:** BIBF 1120 is a potent, orally available triple angiokinase inhibitor that inhibits VEGF receptors (VEGFR) 1, 2, and 3, fibroblast growth factor receptors, and platelet-derived growth factor receptors. This study examined the antitumor effects of BIBF 1120 on hepatocellular carcinoma (HCC) and attempted to identify a pharmacodynamic biomarker for use in early clinical trials.

**Experimental Design:** We evaluated the antitumor and antiangiogenic effects of BIBF 1120 against HCC cell line both *in vitro* and *in vivo*. For the pharmacodynamic study, the phosphorylation levels of VEGFR2 in VEGF-stimulated peripheral blood leukocytes (PBL) were evaluated in mice inoculated with HCC cells and treated with BIBF 1120.

**Results:** BIBF 1120 (0.01 μmol/L) clearly inhibited the VEGFR2 signaling *in vitro*. The direct growth inhibitory effects of BIBF 1120 on four HCC cell lines were relatively mild *in vitro* ($IC_{50}$ values: 2–5 μmol/L); however, the oral administration of BIBF 1120 (50 or 100 mg/kg/d) significantly inhibited the tumor growth and angiogenesis in a HepG2 xenograft model. A flow cytometric analysis revealed that BIBF 1120 significantly decreased the phosphotyrosine (pTyr) levels of VEGFR2$^+$CD45$^{dim}$ PBLs and the percentage of VEGFR2$^+$pTyr$^+$ PBLs *in vivo*; the latter parameter seemed to be a more feasible pharmacodynamic biomarker.

**Conclusions:** We found that BIBF 1120 exhibited potent antitumor and antiangiogenic activity against HCC and identified VEGFR2$^+$pTyr$^+$ PBLs as a feasible and noninvasive pharmacodynamic biomarker *in vivo*. *Clin Cancer Res; 17(6); 1373–81. ©2010 AACR.*

## Introduction

A number of antiangiogenic inhibitors have been studied in clinical settings, some of which have clearly exhibited a clinical benefit in oncology. Consequently, VEGFs and VEGF receptors (VEGFR) are now well-validated targets in cancer therapy (1). In hepatocellular carcinoma (HCC), 2 recent randomized controlled trials for HCC have reported a clinical benefit of single-agent sorafenib for extending the overall survival in both Western and Asian patients with advanced unresectable HCC (2, 3). On the basis of the clear results of these trials, sorafenib is presently regarded as the standard therapy for HCC.

**Authors' Affiliations:** Departments of [1]Genome Biology and [2]Gastroenterology, [3]Kinki University School of Medicine, Osaka, Japan

**Note:** Supplementary data for this article are available at Clinical Cancer Research Online (http://clincancerres.aacrjournals.org/).

**Corresponding Author:** Kazuto Nishio, Department of Genome Biology, Kinki University School of Medicine, 377-2 Ohno-higashi, Osaka-Sayama, Osaka 589-8511, Japan. Phone: 81-72-366-0221; Fax: 81-72-366-0206. E-mail: knishio@med.kindai.ac.jp

**doi:** 10.1158/1078-0432.CCR-09-2755



Because antiangiogenic inhibitors may achieve therapeutic levels long before toxicities arise compared with conventional cytotoxic chemotherapies, identifying pharmacodynamic biomarkers that accurately reflect the effects of the drug on its known targets are needed (4, 5). Therefore, a wide variety of biomarkers of antiangiogenic inhibitors have been proposed and intensively investigated, including plasma proteins, angiogenesis-related signaling, immunohistochemistry of endothelial cell markers for evaluating microvessel density (MVD), circulating endothelial progenitor/cells, and functional imaging such as dynamic contrast-enhanced MRI and molecular imaging using positron emission tomography (6). These candidate biomarkers have been evaluated and characterized as prognostic, pharmacodynamic, or response-predictive markers. Although the utility of biomarkers for evaluating MVD was highly anticipated, these markers were not predictive for clinical response in patients treated with bevacizumab (7). Regarding growth factors and cytokines, the plasma VEGF level has been shown to be neither a pharmacodynamic nor a predictive biomarker of antiangiogenic drugs (7, 8), although the plasma VEGF level is a well-known prognostic biomarker (9–11). Plasma-soluble VEGFR2, on the other hand, may be a promising and specific biomarker of